FACULDADE DE CIÊNCIAS E TECNOLOGIA DA UNIVERSIDADE DE COIMBRA

Radiobiology of Malignant Melanoma

Melanin Behavior in Gamma Radiation Induced Oxidative Stress and Genotoxicity: Implications for Radiotherapy

Sérgio Manuel Lopes da Fonseca

2009

Integrated Masters of Science Biomedical Engineering Project

FACULDADE DE CIÊNCIAS E TECNOLOGIA DA UNIVERSIDADE DE COIMBRA

Radiobiology of Malignant Melanoma

Melanin Behavior in Gamma Radiation Induced Oxidative Stress and Genotoxicity: Implications for Radiotherapy

Sérgio Manuel Lopes da Fonseca

2009

Scientific Advisors:

Margarida Goulart de Medeiros, PhD

Célia Gomes, PhD

Acknowledgements

The author would like to thank Dr. Margarida Goulart for all motivation, support and transmitted knowledge during this last year of work. He likes also to thanks Dr. Célia Gomes.

The entire experimental work included in this project was performed in laboratory facilities of the Dosimetry and Radiobiology Group of the Unit of Radiological Protection and Safety - Nuclear and Technological Institute (ITN), so the author would like to thank ITN's President, Dr. Júlio Montalvão e Silva, Group and Unit supervisors, Dr. Pedro Vaz and Dr. Maria Berta Martins, all the group colleagues with a special thanks to Catarina Antunes for her help during the initial laboratory training.

The author is also deeply thankful to ITN's Chemical Department, particularly Dr. Lurdes Gano and Dr. Isabel Rego dos Santos, for kindly supplying the B16-F1 cells which were critical for the success of the project, and to ITN's Metrological Laboratory of Ionizing Radiation and Radioactivity, particularly Dr. Carlos Oliveira, Group Supervisor, and Dr. João Cardoso and Dr. Luis Santos, for providing all the help and technical support for the gamma irradiations of the samples.

At last a very special thanks to my parents and Filipa for all the love and support.

Table of Contents

List of Figures

List of Tables

List of Abbreviations

AECL	Atomic Energy of Canada, Ltd.
AIDS	Acquired immunodeficiency syndrome
ALM	Acral lentiginous melanoma
AML	Acute myeloid leukemia
BCC	Basal cell carcinoma
BHT	Butilhydroxytoluene
BN	Binucleated cell
CBMN	Cytokinesis-block micronucleus
CCL	Chronic lymphocytic leukemia
CI	Confidence interval
Cyt-B	Cytochalasin-B
DMEM	Dulbecco's Modified Eagle's Medium
DMSO	Dimethil sulfoxid
DNA	Deoxyribonucleic acid
FBS	Foetal Bovine Serum
IR	Ionizing Radiation
LMM	Lentigo maligna melanoma
MDA	Malondialdehyde
MM	Malignant Melanoma
MNi	Micronucleus/micronuclei
MTT	3-(4,5-dimethylthiazol-2-yl)-2,5-diphenyltetrazolium bromide
NM	Nodular melanoma
PBS	Phosphate-buffered saline
PCA	Perchloric acid
ROS	Reactive oxygen species
SCC	Squamous cell carcinoma
SD	Standard deviation
SIR	Standardized incidence ratio
SMR	Standardized mortality ratio
SSM	Superficial spreading melanoma
TBA	Thiobarbituric acid
TEM	Transmission Electron Microscopy
UV	Ultra Violet Radiation

Abstract

The goals of the present work are to evaluate the sensitizing/protective effect of melanin in the cytotoxicity and genotoxicity of ionizing radiation, including induced oxidative stress modulation in malignant melanoma cells in presence and absence of melanin, and to interpret obtained results in the perspective of melanoma or other malignancies radiotherapy.

An overview about the generality of skin cancers with special attention to malignant melanoma is presented. Skin cancer incidence has been steadily increasing over the last 40 years; however the mortality has been decreasing, mainly due to early diagnosis and prevention campaigns. Although malignant melanoma (MM) represents only 7% of total number of skin cancers, it is responsible for more than 80% of deaths attributable to skin cancers. MM presents higher incidence rates in light skinned populations, and in individuals chronically exposed to the sun, but a relatively high MM incidence has been reported in subjects exposed to ionizing radiation (IR), indicating that may there to be a causal relationship between MM and IR.

The biological effects of ionizing radiation interaction are explored with special focus on the biologic effects of radiation in normal and melanoma cells and the interaction of melanin with the damage caused by IR. Melanin is a class of pigments present in almost all living beings. Melanin protection against UV radiation is widely acknowledged, but not completely understood; some recent studies claim that melanin can also play an in important role in protection against ionizing radiation. However, other studies evidenced that melanogenesis, the process by which melanocytes produce melanin, may be a source of reactive substances, some of them carcinogenic. This study is an attempt to clarify which behavior prevails in IR-exposed cells.

In this work B16-F1 cells (mouse melanoma line) were irradiated at 1.5 Gy in the presence and absence of several concentrations of melanin, either added to the medium or obtained by melanogenesis induction using different concentrations of L-tyrosine as a precursor during cell growth. To assess genotoxic effects, cytocinesis-block micronucleus assay was performed. MTT assay reveals the level of cytotoxicity and cell death by comparing control and irradiated cell ability to reduce MTT salt to formazan (only metabolically active cells are able to complete this process). Lipid peroxidation may result from the indirect action of IR, by the intermediate reactive oxygen species generated in the intracellular and extracellular medium. Lipid peroxidation products were quantified in the supernatant of cell cultures by the thiobarbituric acid reaction, expressed as malondialdehyde, as a measure of oxidative stress MDA-TBA reaction assay giving an idea of oxidative stress products production.

The obtained results strongly suggest that melanin may play an important role in protection against ionizing radiation. This conclusion provides a partial explanation as to why MM has a strong radiotherapy resistance; however melanin could be applied in melanin-based radioprotective materials, suitable for internal administration to prevent side effects in normal tissues during radiotherapy.

Future prospects include an investigation on melanin behaviour when irradiated with particulate ionizing radiation. It would also be interesting to attempt to develop biomaterials similar to melanosomes, in the form of nanospheres, enabling the internal administration of melanin, via intravenous injection, for instance, to test melanin protection *in vivo.*

Resumo

Os objectivos do presente trabalho são: avaliar o efeito sensibilizante ou protector da molécula de melanina na citotoxicidade e genotoxicidade da radiação ionizante, investigar a modulação do stress oxidativo radioinduzido em células de melanoma maligno na presença e ausência de melanina e interpretar os resultados na perspectiva da radioterapia do melanoma ou outras neoplasias malignas.

É ainda apresentada uma revisão bibliográfica acerca dos cancros cutâneos com especial atenção para o melanoma maligno (MM). A incidência do cancro da pele tem vindo a aumentar nos últimos 40 anos, porém a mortalidade tem diminuído, principalmente graças às campanhas de sensibilização para os sinais de alerta, que conduzem a um diagnóstico mais precoce e com melhor prognóstico. No conjunto dos cancros da pele, embora o MM represente apenas 7% da totalidade de casos, é responsável por mais de 80% das mortes atribuíveis a esta neoplasia: para tal contribui o seu carácter invasivo e a sua resistência aos tratamentos por radio e quimioterapia. O MM apresenta maior incidência em populações onde predominam fotótipos de pele clara, entre outros factores de risco incluindo exposição crónica a radiação UV, no entanto foi também notada uma taxa de incidência aparentemente aumentada em indivíduos expostos a radiação ionizante, indicando uma possível relação causal entre a radiação ionizante e o MM.

Neste trabalho explora-se a interacção da radiação ionizante com células eucariotas, com principal incidência nos efeitos radiobiológicos e na interacção com a molécula de melanina. A melanina é uma classe de pigmentos presente na maior parte dos seres vivos. São largamente conhecidas as propriedades protectoras da melanina contra a radiação UV, apesar de não estarem completamente explicadas; paralelamente, alguns estudos recentes sugerem que a melanina pode apresentar também propriedades radioprotectoras. Contudo, outros autores apontam a melanogénese (processo pelo qual os melanócitos produzem melanina) como potencial fonte de substâncias citotoxicas, algumas delas carcinogénicas. O presente trabalho tenta contribuir para clarificar qual a acção da melanina que prevalece em células de MM expostas a radiação ionizante.

Para este trabalho foram irradiadas células B16-F1 de melanoma de ratinho com uma dose aguda de radiação gama de 1,5 Gy com diferentes concentrações de melanina no meio de cultura, obtidas quer por adição de melanina ao meio, quer por indução/inibição da produção de melanina na presença e ausência de L-tirosina durante o crescimento celular. Para avaliar os efeitos genotóxicos procedeu-se ao ensaio do micronúcleo com citocinese bloqueada. A toxicidade aguda foi avaliada pelo ensaio do MTT que quantifica a viabilidade celular, comparando a capacidade das células de controlo e irradiadas de reduzir o sal MTT para formazan (composto corado). Avaliou-se ainda a peroxidação lipídica resultante da acção das espécies reactivas geradas no meio intra e extracelular devido à exposição a radiação ionizante. Quantificaram-se os produtos de peroxidação lipídica, que reflectem o stress oxidativo da amostra, através da reacção com o ácido tiobarbiturico (TBA), sendo expressos em equivalentes de malondialdeído (MDA).

Os resultados obtidos sugerem fortemente que a melanina exerce um papel importante na protecção contra a radiação ionizante. Este facto contribui para explicar a grande radiorresistência do MM perante a radioterapia; porém a melanina poderia ser usada na produção de materiais radioprotectores passíveis de administração intracorporal de modo a proteger os tecidos saudáveis dos efeitos colaterais da radioterapia.

De futuro aconselha-se investigar o comportamento da melanina quando irradiada com radiação particulada. Seria também interessante o desenvolvimento de biomateriais semelhantes a melanossomas, tais como nanoesferas, permitindo administrar melanina internamente, por exemplo por via intravenosa, permitindo experiências *in vivo.*

Objectives

The objectives of this work are:

- To study melanin sensitizing/protective effects in cytotoxicity and genotoxicity induced by ionizing radiation

- To evaluate oxidative stress modulation in malignant melanoma cells in the presence and absence of melanin

- To interpret the results in the perspective of radiotherapy success in malignant melanoma or other neoplasic malignancies.

Skin Cancer and Melanoma

Skin cancer is the more frequent malignancy among Caucasian individuals. Its incidence has been steadily increasing over the last 40 years (J. A. Amaro 2009). Early treatment is usually simple with high rates of cure (> 90%). However, advanced stages of the disease require complex and expensive treatment with relatively reduced cure probability, possibly ending with death of the patient. Prevention is, therefore, the best practice:

- Primary prevention – the main causal factors are well known and potentially avoidable;
- Secondary prevention or early diagnostic - skin is an easily accessible organ for direct observation so detection of skin cancer at early stages is possible and enables a good prognosis.

Skin cancer has low global mortality rate due to a highly efficient early diagnostic and treatment. However, its importance should not be underestimated: this disease has a high aggressiveness and morbidity, with a deep negative impact in patients' and their families' quality of life.

Skin Cancer Types

Skin cancers are divided essentially in three groups:

1. Keratinocytic or epidermal carcinomas, derived from epidermal keratin-producer cells including:
    a. Basal cell carcinoma or basilioma (BCC);
    b. Squamous cell or spino-cellular carcinoma (SCC);
2. Malignant Melanoma (MM), derived from melanin-producer cells, the melanocytes;
3. Other skin malignancies, including skin lymphomas and Kaposi sarcoma.

Incidence has been increasing in all kinds of skin cancer; especially in MM. Epidermal carcinomas are, by far, the most frequent skin tumors, representing about 90% of all kinds of skin cancers, 65% corresponds to BCC and 25% to SCC. MM represents about 7% and 3% to other tumors heterogenic group (Table 1 and Fig. 1) (J. A. Amaro 2009).

Table 1 - Relative incidence of skin cancer types (J. A. Amaro 2009)

Skin cancer types	Incidence (%)
BCC	65
SCC	25
MM	7
Other Tumors	3

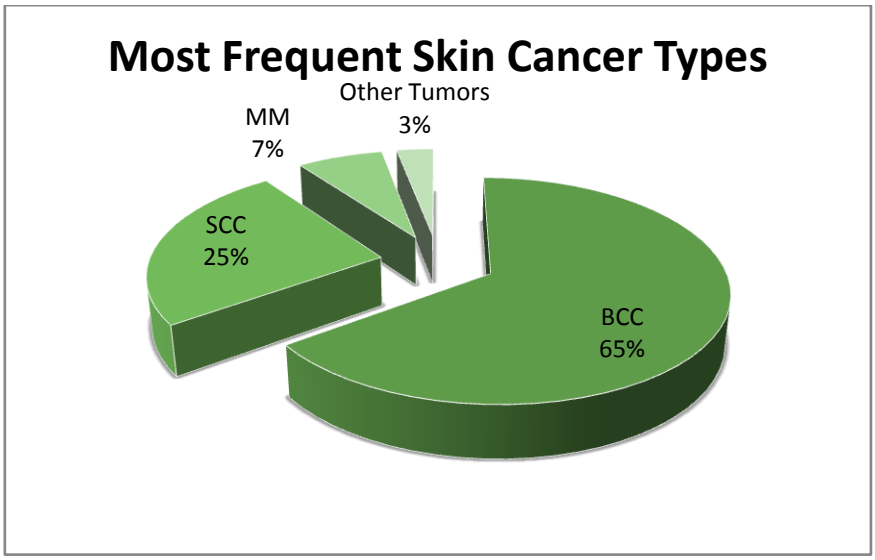

Fig. 1 - Relative frequency of skin cancer types (J. A. Amaro 2009). BCC Basal Cell Carcinoma; SCC – Squamous Cell Carcinoma; MM – Malignant Melanoma.

Despite MM represent only 7% of the total number of skin cancers; it is responsible for more than 80% of deaths attributable to this malignancy. It is ten times more frequent today than in the 60's and its incidence has more than duplicated in the last 15 years and its trend is for a continuous increase (J. A. Amaro 2009).

Occupational chronic sun exposure is the main etiology for BCC and SCC; however people with acute sun exposure are at higher risk of MM, usually caused by coastal sun exposure (Ribas dos Santos 2009).

Non Melanoma Skin Cancers

As previously stated, epidermal carcinomas are, by far, the most frequent skin cancers, representing about 90% of all malignant skin tumors. This type of skin cancer mainly affects light-skinned populations, with low incidence in Asians and Latin-Americans, and a very low frequency in Negroid population (World Health Organization 2008). Basal cell carcinoma and squamous cell carcinoma are the two main forms of epidermal, non-melanoma skin cancer.

SCC occurs almost always in chronically sun-exposed skin areas, whereas BCC may also occur in areas exposed to the sun only intermittently. Non-melanoma skin cancers have higher incidence in Caucasian populations residing in areas close to Equator (Australia), showing an important variability between Europe, the USA and Australia: incidence rates are about 5 times higher in the USA and 20-40 times higher in Australia than in Europe (World Health Organization 2008).

BCC and SCC are slow-growing tumors that are locally invasive, rarely resulting in distant metastasis.

Basal Cell Carcinoma or Basilioma (BCC)

BCC is the most frequent skin cancer; its incidence is listed in Table 2. Its origin is in the basal layer of the epidermis and it mostly affects Caucasian individuals chronically exposed to the sun: agricultural workers, fishermen, construction workers, etc. More often, this kind of cancer manifests itself after the 4th decade of life, and preferentially in most exposed body

areas such as face, neck and torso. It may present itself as a slow-growing, shinning and pink node or superficial wound, with no apparent cause and no spontaneous healing tendency (J. Amaro 2009).

BCC is a localized only invasive tumor, not metastatic. Treatment in early stages is very simple (surgery, cryosurgery and laser) with good prognosis (healing rates higher than 95%). It may become more aggressive in later stages, invading surrounding tissues and causing permanent damages and mutilations in certain anatomical areas (nose, ear, eyelid, etc.). Even in these advanced stages cure is often possible with surgery and radiotherapy (J. Amaro 2009).

Squamous cell carcinoma (SCC)

SCC is the second most frequent skin cancer; its incidence is listed in Table 2. Its origin is in the stratified *spinosum* squamous epithelium cells and it is most frequent among the same population as BCC, but at elder ages: its incidence increases with age (exponential increase, doubling in last 25 years of the individual's life span) and in patients with more sun-aged skin, preferentially in the most exposed body areas such as face, neck, back of the hands and legs. It appears almost always over pre-existing lesions or in patients chronically exposed to carcinogenic agents (tobacco, X-rays, arsenic, tar and derivatives) (J. Amaro 2009). It's estimated that SCC's incidence will continue to increase due to population aging and environmental factors like ozone layer deterioration (J. A. Amaro 2009).

SCC is more aggressive and faster growing than BCC, being responsible for the majority of non melanoma skin cancer mortality, accounting for around 75% of all non-melanoma skin cancer deaths (World Health Organization 2008). In most cases it's manifested as a fast growing node, with ulcer and bleeding tendency. In addition to being locally invasive it may metastise, however, with early diagnostic, has high chances of cure (J. A. Amaro 2009). Despite the increasing incidence, SCC mortality (Fig. 2) has decreased 20% in last 20 years in Portugal mainly due to early diagnosis and treatment, consequences of the better national medical coverage and information campaigns after 1988 (J. A. Amaro 2009).

Table 2 - Incidence rates in several countries, per year and per 100.000 inhabitants (J. A. Amaro 2009)

Country	Basal Cell Carcinoma (BCC)		Squamous Cell Carcinoma (SCC)	
	Men	Women	Men	Women
Australia	2024	1579	1035	472
U.S.A.	247	150	65	24
United Kingdom	112	54	32	6
Portugal	85	65	19	11
Switzerland	52	38	16	8
Finland	49	45	9	5

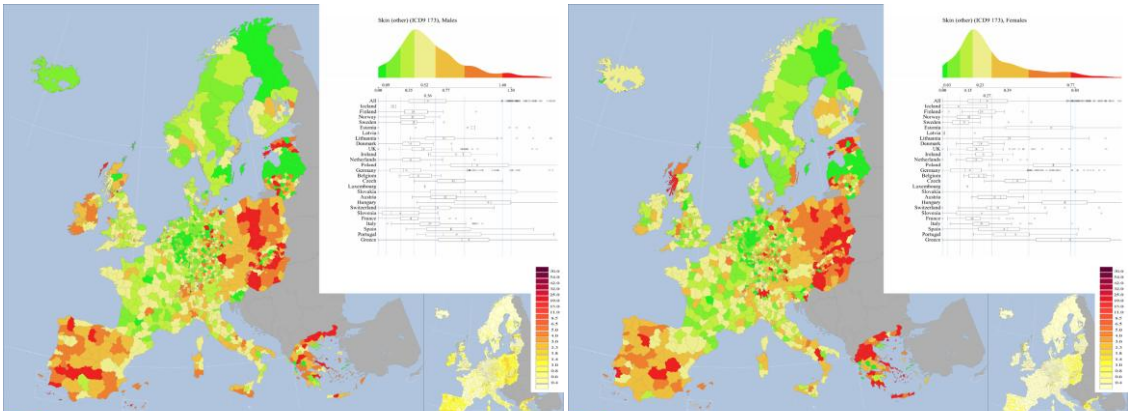

Fig. 2 - Mortality rates from non-melanoma skin cancer for men (left) and women (right) in Europe between 1993-1997[1] (World Health Organization 2008).

BCC and SCC risk factors

Adapted from: (J. A. Amaro 2009)

Environmental factors

- Sun exposure (UVA and UVB)
- Artificial UV tanning
- Ionizing radiation (occupational, medical, accidental)

Chemical agents

- Arsenic (industrial, environmental, drugs)
- Polycyclic aromatic hydrocarbons (oil and tar derivatives)
- Tobacco

Biological agents

- Human papillomavirus (HPV)

Genetic factors

- Bright skin (Phototypes I and II)
- Genodermatosis
    - Albinism
    - Xeroderma pigmentosa (autosomal recessive genetic disorder of DNA repair in which the ability to repair damage caused by UV light is deficient)
    - Nevoid Basal Cell Carcinoma Syndrome (autosomal dominant condition that can cause unusual facial appearances and a predisposition for basal cell carcinoma)

Immunosuppression

- Organ transplant
- Cancer treatments
- AIDS

[1] European Community including countries of the EFTA (Switzerland, Iceland and Norway). The main map represents the relative distribution of rates using a scale from lower rates in green to highest rates in red using percentiles of the distribution of rates. The second map represents the distribution of rates using an absolute scale and the upper right sub-Figure contains the distribution of rates and boxplots of rates by country.

Other skin tumors

Besides epidermal carcinomas and melanoma, there are an enormous variety of other skin cancers (Table 3), much less frequent, and whose origin does not seem to be related to sun exposure.

Table 3 - Other non-melanoma cutaneous malignancies (Harrison's 2005)

Tumor Type	Most common location	Recurrence rate, %	Metastatic rate, %
Atypical fibroxanthoma	Head and neck	21	4
Merker cell carcinoma	Head and neck	40	75
Dermatofibrosarcoma protuberans	Trunk	50	1
Sebaceous carcinoma	Eyelid	12	30
Microcystic adnexal carcinoma	Face	50	1 case
Porocarcinoma	Extremity	20	10
Eccrine carcinoma	Head and neck	36	11
Angiosarcoma	Head and neck	75	75

In this heterogeneous group it is worth to refer skin lymphomas and Kaposi sarcoma.

Skin lymphomas

Lymphatic system cancers that primary appear at skin level with still unknown etiology. There are two major types:

1. T-lymphocytes skin lymphomas: some tumors look like mushrooms, so its classic clinic form is called “fungous mycosis”.
2. B-lymphocytes skin lymphomas: low malignancy lymphomas, however generally higher malignancy than T-lymphomas.

Treatment varies with disease’s stage; includes often photo-chemotherapy (UV exposure after photosensitizing drug ingestion), interferon immunotherapy, radiotherapy and chemotherapy (J. Amaro 2009).

Kaposi sarcoma

This kind of cancer targets primarily skin and mucosae, and shows an appearance of multiple spots and red-violet nodes. It was, until recently, a relatively rare disease, affecting mainly the inferior limbs of males over 50 years of age, in Mediterranean and African countries, where it is an endemic disease. However, with the growing number of cases of acquired immunodeficiency syndrome (AIDS), the incidence of Kaposi sarcoma exponentially increased, frequently affecting patients with AIDS. Although in the classic variant the disease evolution is relatively slow and with good prognosis, when associated with AIDS it has a fast evolution and is more aggressive. In early stages, radiotherapy is an efficient treatment in localized lesions; in later stages chemotherapy is needed. Recent studies seem to point to Herpes virus type 8 (HSV-8) as probable etiology (J. Amaro 2009).

Malignant Melanoma

History

The first report of a melanoma was by Hippocrates in the 5th century B.C. The next reference we can find is by Rufus of Ephesus (60? - 120?), a Greek physician widely known among the ancients for his descriptions of the meninges, the crystalline lens, the optic chiasm, the synchronism of the heart beat and the pulse, filariasis, gout and certain cancers of the skin, notably melanoma (Urteaga and Pack 1966).

Although melanoma is not a new disease, evidence for its occurrence in antiquity is rather scarce. However, one example lies in a 1960s examination of nine Peruvian Inca mummies, radiocarbon-dated to be approximately 2400 years old, which showed apparent signs of melanoma: melanotic masses in the skin and diffuse metastases to the bones (Fig. 3). (Urteaga and Pack 1966)

Fig. 3 - A and B. Pre-Colombian Inca skulls containing metastatic melanoma in bone (Urteaga and Pack 1966).

John Hunter (a Scottish surgeon regarded as one of the most distinguished scientists and surgeons of his day, the Hunterian Society of London was named in his honor) is reported to be the first to operate on metastatic melanoma in 1787. Although not knowing precisely what it was, he described it as a "cancerous fungous excrescence". The excised tumor was preserved in the Hunterian Museum of the Royal College of Surgeons of England. It was not until 1968 that microscopic examination of the specimen revealed it to be an example of metastatic melanoma (Bodenham 1968).

Eiselt, in 1861-1862, discussing pigmented tumors, stated that the description of “fatal black tumors with metastases and black fluid in the body” can be found in Highmore (1651), Bartholin (1677), Bonet (1679), and Henrici and Nothnagel (1757).The French physician René Laennec was the first to describe melanoma as a disease entity. His report was initially presented during a lecture for the Faculté de Médecine de Paris in 1804 and then published as a bulletin in 1806. Robert Carswell, in 1838, first employed the term melanoma to designate these pigmented malignant tumors (Urteaga and Pack 1966).

The first formal acknowledgment that advanced stages of melanoma are untreatable came from Samuel Cooper in 1840. He stated that 'the only chance for benefit depends upon the early removal of the disease ...' (Cooper 1840) More than one and a half centuries later this situation remains largely unchanged.

Epidemiology

MM has an incidence of about 160 000 new cases worldwide each year (approximately 79 000 males and 81 000 women), of which almost 80% are in Oceania, Europe and North America (Fig. 4) (World Health Organization 2008). On a global scale, MM is the 16th and 15th most commonly diagnosed cancer in males and females (respectively), but has significant regional variation, with higher incidence in Australia and New Zealand (4th most common males, 3rd in females), North America (6th in males, 5th in females) and Europe (16th in males, 8th in females) (World Heath Organization 2006).

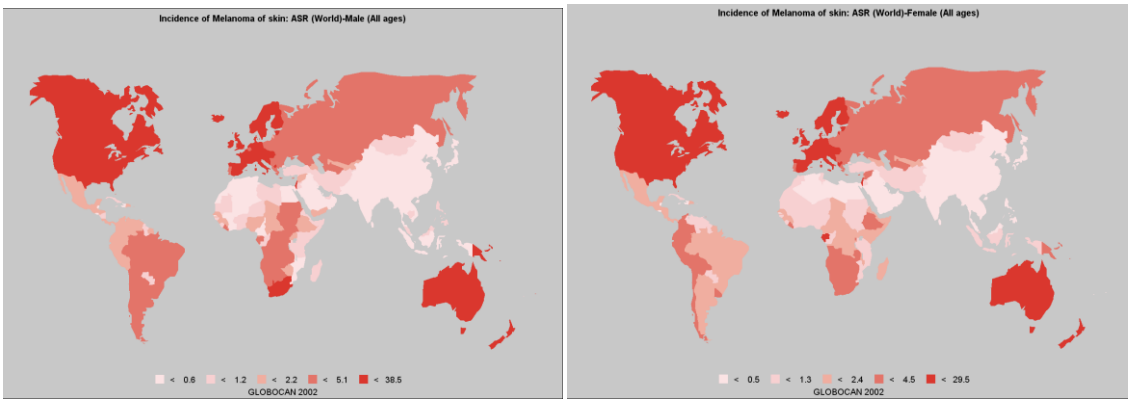

Fig. 4 - Incidence of melanoma worldwide in men (left) and women (right) at all ages (World Health Organization 2008)

The highest incidence of melanoma occurs in Australia where the population is predominantly Caucasian, mostly Northern European descendents. In Western Europe incidence rates are higher in the North than in the South (Fig. 5) (World Heath Organization 2006) reflecting the protective effect of melanin presence in the southern populations. U.S. caucasoids have rates 15 times higher than U.S. negroids, and a similar contrast is observed in South Africa and Zimbabwe. Melanoma is also relatively uncommon among Asians and Central/South American populations (Table 4 and Figure 6).

Table 4 - Melanoma incidence in several world countries (J. A. Amaro 2009)

Country	Incidence rate per 100.000 inhabitants	
	Men	Women
Australia, Queensland	51.1	38.1
Australia, South New Wales	36.9	25.9
New Zealand	32.8	30.6
U.S.A	15.4	11.6
Sweden	11.8	11.9
Israel	11.7	11.3
Denmark	10.5	13.4
Netherlands	8.0	10.9
Czech Republic	8.1	7.9
Scotland	7.1	9.9
England	5.8	7.4
Germany	6.3	6.1
Spain	4.1	5.4
Portugal	3.8	5.0
Japan	0.4	0.5
China	0.3	0.2
India	0.3	0.2

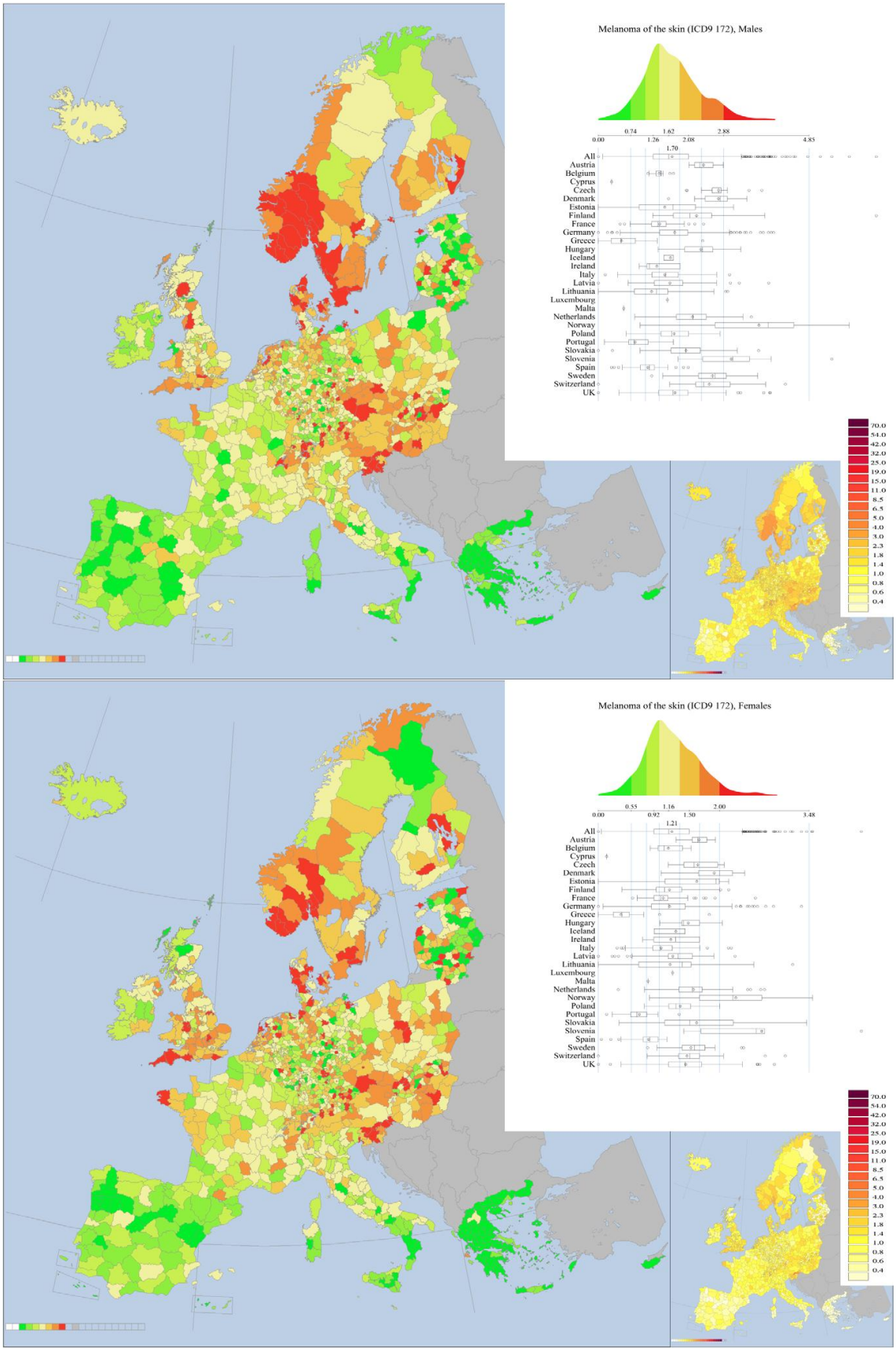

Fig. 5 The prominent features of the geographical distribution of melanoma in men (top) and women (bottom) are the high levels across (southern) Finland, Norway, Sweden and Denmark and into northern Germany and The Netherlands, in Austria, Switzerland, the Czech Republic, Slovakia, Hungary and Slovenia, and in southern England. Rates were low in most of Spain, Portugal, southern Italy and Greece (World Health Organization 2008)

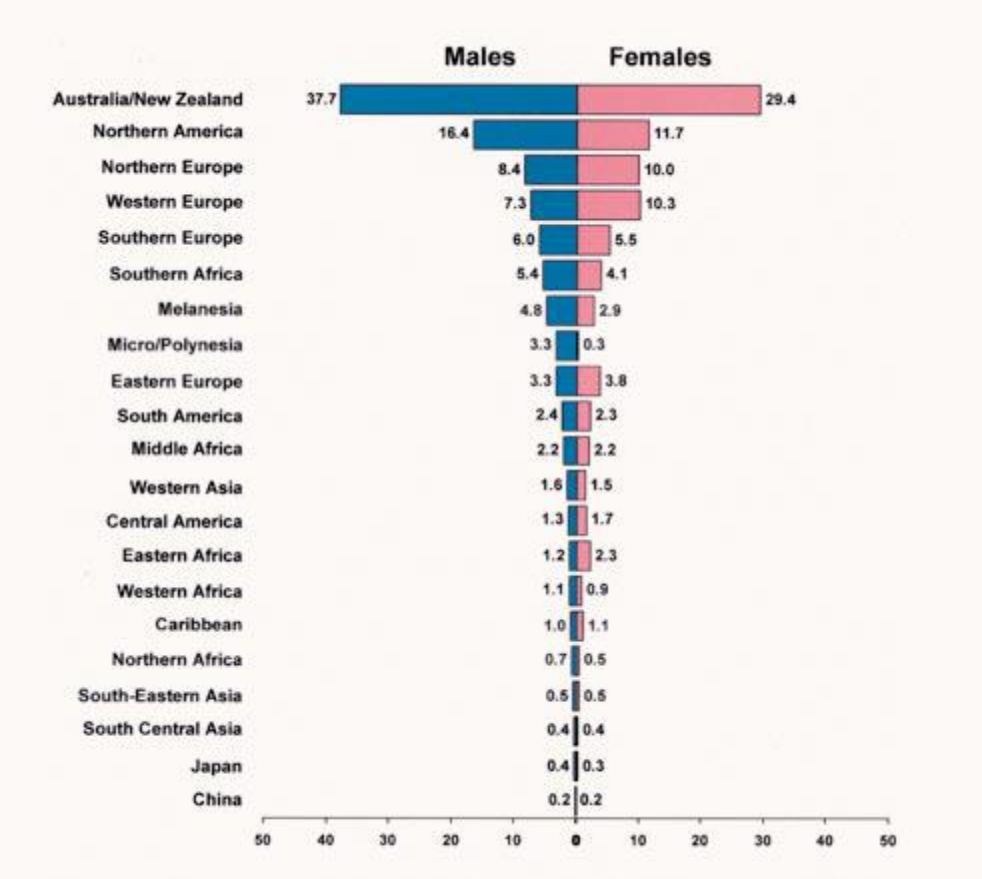

Fig. 6 Age-standardized incidence rates for MM, per 100 000 inhabitants and year, adjusted to the world standard population (World Heath Organization 2006)

Increasing incidence rates do not correspond to equivalent increasing mortality rates. This difference may be due to an earliest MM diagnostic and treatment, with good prognosis, or it may also be consequence of the worldwide prevention campaigns in the last 20 years

Clinical Characteristics

With rare exceptions, MM arises from atypical melanocytes situated along the dermal – epidermal junction (*stratum basale* of epidermis). MM *in situ* is confined to the epidermis, where there are neither blood vessels nor lymphatic vessels to enable metastases transport. When MM invades the dermis it gains access to vasculature (Cohen, et al. 2008).

There are four main types of MM (Table 5). Three of these – superficial spreading melanoma (SSM), lentigo maligna melanoma (LMM) and acral lentiginous melanoma (ALM) – are characterized by a biphasic growth pattern: the lesion has a period of slower superficial (so-called “radial”) growth phase, succeeded by a more rapid, invasive “vertical” growth phase. During radial growth phase, lesion increases in size but does not penetrate deeply, undergoing centrifugal enlargement, and tending to be relatively flat. This period may persist for years, during which MM develops little, if any, tendency to metastise. It is during this period that MM has more chances of cure by surgical excision (Cohen, et al. 2008 and Harrison's 2005).The vertical growth phase appears to represent a new and distinct clone of tumor cells: the dome-shaped nodule grows rapidly. During this invasive growth phase, the neoplasm penetrates the connective tissue, accessing blood and lymphatic vessels and resulting in metastasis. Nodular Melanoma (NM) exhibits a monophasic growth pattern, not having a recognizable radial

growth phase and usually presenting a vertical growth as a deeply invasive lesion from the outset, capable of early metastasis (Cohen, et al. 2008 and Harrison's 2005). The two growth phases are schematically represented in Fig. 7.

Table 5 - Clinical features of the most common types of MM (Cohen, et al. 2008 and Harrison's 2005).

Clinical feature	Lentigo maligna melanoma (LMM)	Superficial spreading melanoma (SSM)	Nodular melanoma (NM)	Acral lentiginous melanoma (ALM)
Frequency in caucasoids	≈ 10%	≈ 70%	≈ 10%	≈ 5%
Site	Sun-exposed surfaces, particularly malar region of cheek and temple	Any site (more common on upper back and, in women, on lower legs)	Any site	Palm sole, nail bed, mucous membrane
Average age at diagnosis, years	70	40-50	40-50	60
Margin	Flat	Distinctly palpable	Palpable: spheroid	Flat
Color	In flat portions, shades of brown and tan predominant, but whitish gray occasionally present; in nodules, shades of reddish-brown, bluish black	Shades of brown mixed with bluish red (violaceous), bluish black, reddish brown, and often whitish pink, and the border of lesions is at least part visibly and/or palpably elevated	Reddish blue (purple) or bluish black; either uniform in color or mixed with brown or black	In flat portions, dark brown predominantly; in raised lesions (plaques) brown-black predominantly
Growth pattern	Biphasic – radial phase: lentiginous spread 5-20 years; vertical phase: rapid invasion of dermis over weeks to months	Biphasic – radial phase: pagetoid spread 1-12 years; rapid invasion of dermis over weeks to months	Monophasic – vertical phase from the outset; tumor present months to 2 years at time of diagnosis	Biphasic – radial phase: 1-10 years, of various histology; rapid invasion of dermis over weeks to months

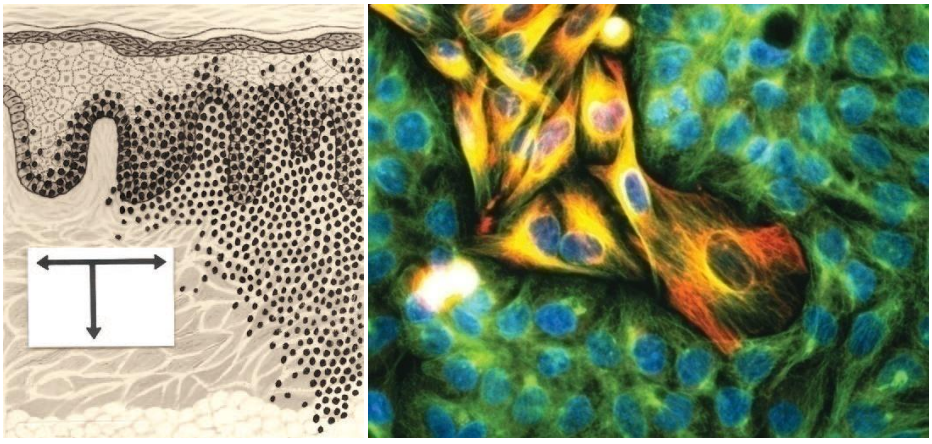

Fig. 7 – *Left* - Schematic representation of biphasic growth pattern. In radial growth phase, atypical melanocytes proliferate along the dermal–epidermal junction along a horizontal plane. In the vertical growth phase, atypical melanocytes penetrate toward deeper tissue levels. (Cohen, et al. 2008) *Right* - Imunoflourescent light micrography of melanoma cells (yellow) invading skin epithelial cells (green). (melanoma. [Photograph] n.d.)

Risk factors for Malignant Melanoma

Adapted from (J. A. Amaro 2009)

Constitutionals (Phenotypic) Factors

1. *Phototype (skin pigmentation capacity)*

- Bright skin (phototypes I and II)
- Freckles formation tendency
- Red or blond hair
- Blue eyes

2. *Melanocytic nevi number, size and shape*

- More than 50 nevus
- Diameter equal or bigger than 6mm
- Congenital giant nevi
- Atypical or dysplastic nevi

Genetic (genotypic) factors

Tumor activity suppressing genes mutations:

- CDKV-2A and p53 genes mutations in sporadic melanoma
- P16 and BRAF genes mutations in familiar melanoma
- DNA repair defects (Xeroderma pigmentosa)

Environmental factors

- Intense and intermittent sun exposure (UVA and UVB)
- Solar burns in childhood and adolescence
- Artificial UV tanning
- Ionizing radiation (occupational, medical, accidental)

Immunosuppression

- Organ transplant
- Cancer treatments
- AIDS

Personal and familiar history

Prognostic factors

The most important prognostic factor is the stage at the time of presentation. Fortunately, most melanomas are diagnosed in clinical stages I and II. The revised staging system for melanoma is based on microscopic primary tumor depth (Breslow's thickness), presence of ulceration, evidence of nodal involvement, presence of microscopic satellites and presence of metastatic disease (Fig. 8) (Harrison's 2005).

TNM classification[1,2]

T – Primary tumour

The extent of the tumour is classified after excision, see pT.

N – Regional lymph nodes

- NX Regional lymph nodes cannot be assessed
- N0 No regional lymph node metastasis
- N1: Metastasis in one regional lymph node
  - N1a: only microscopic metastasis (clinically occult)
  - N1b: macroscopic metastasis (clinically apparent)
- N2: Metastasis in two or three regional lymph nodes or intralymphatic regional metastasis
  - N2a: only microscopic nodal metastasis
  - N2b: macroscopic nodal metastasis
  - N2c: satellite or in-transit metastasis *without* regional nodal metastasis
- N3: Metastasis in four or more regional lymph nodes, or matted metastatic regional lymph nodes, or satellite or in-transit metastasis *with* metastasis in regional lymph node(s)

Note: Satellites are tumour nests or nodules (macro- or microscopic) within 2cm of the primary tumour. In-transit metastasis involves skin or subcutaneous tissue more than 2 cm from the primary tumour but not beyond the regional lymph nodes.

M – Distant metastasis

- MX Distant metastasis cannot be assessed
- M0 No distant metastasis
- M1 Distant metastasis
  - M1a: Skin, subcutaneous tissue or lymph node(s) beyond the regional lymph nodes
  - M1b: Lung
  - M1c: Other sites, or any site with elevated serum lactic dehydrogenase (LDH)

pT – Primary tumour (pathological classification)

- pTX Primary tumour cannot be assessed*
- pT0 No evidence of primary tumour
- pTis Melanoma in situ (Clark level I) (atypical melanocytic hyperplasia, severe melanocytic dysplacia, not an invasive malignant lesion)
- pT1: Tumour 1mm or less in thickness
  - pT1a: Clark level II or III, without ulceration
  - pT1b: Clark level IV or V, or with ulceration
- pT2: Tumour more than 1mm but not more than 2mm in thickness
  - pT2a: without ulceration
  - pT2b: with ulceration
- pT3: Tumour more than 2mm but not more than 4mm in thickness
  - pT3a: without ulceration
  - pT3b: with ulceration
- pT4: Tumour more than 4mm in thickness
  - pT4a: without ulceration
  - pT4b: with ulceration

Note: *pTX includes shave biopsies and regressed melanomas.

Stage grouping[3]

Stage 0	pTis	N0	M0
Stage I	pT1	N0	M0
Stage IA	pT1a	N0	M0
Stage IB	pT1b	N0	M0
	pT2a	N0	M0
Stage IIA	pT2b	N0	M0
	pT3a	N0	M0
Stage IIB	pT3b	N0	M0
	pT4a	N0	M0
Stage IIC	pT4b	N0	M0
Stage III	Any pT	N1, N2, N3	M0
Stage IIIA	pT1a-4a	N1a, 2a	M0
Stage IIIB	pT1a-4a	N1b, 2b, 2c	M0
	pT1b-4b	N1a, 2a, 2c	M0
Stage IIIC	pT1b-4b	N1b, 2b	M0
	Any pT	N3	M0
Stage IV	Any T	Any N	M1

[1] UICC (2002). TNM classification of malignant tumours. Sixth edition. Wiley, New York
[2] AJCC (2002). Cancer staging manual. Sixth edition. Springer, New York
A help desk for specific questions about the TNM classification is available at http://www.uicc.org (activities, TNM)
[3] Clinical staging includes complete excision of the primary melanoma [pT] with clinical/radiological assessment for regional and distant metastases. Pathologic staging includes complete excision of the primary melanoma [pT] and pathologic assessment of the regional lymph nodes [pN] after partial or complete lymphadenectomy. Stage 0 or stage IA patients do not require pathological evaluation of their lymph nodes.

Fig. 8 - TMN classification of MM (World Heath Organization 2006)

MM may recur after many years. About 10 to 15% of first-time recurrences develop >5 years after treatment of the original lesion. The time to recurrence varies inversely with tumor thickness. An alternative prognostic scheme for clinical stages I and II melanoma, proposed by Clark, is based on the anatomical level of invasion of the skin: level I is intra-epidermal (*in situ*); level II penetrates the papillary dermis; level III spans the papillary dermis; level IV penetrates the papillary dermis and level V penetrates into the subcutaneous fat. The 5-year survival for these stages averages 100, 95, 82, 71 and 49%, respectively (Harrison's 2005).

The aim of differential diagnosis is to distinguish benign pigmented lesions from melanoma and its precursors. If melanoma is a consideration, then biopsy is appropriate. Alarm signals that may indicate appearance of MM are: new dark brown mole or mole arising; alterations in a pre-existing mole (size, thickness, color, border, burning or itch sensation).

Early detection of melanoma may be facilitated by applying the "ABCD rules" (J. A. Amaro 2009) to distinguish benign acquired nevi forms from clinically atypical moles, potential melanoma precursors:

A. asymmetry, benign lesions are usually symmetric;
B. border irregularity, most nevi have clear-cut borders;
C. color variegation, benign lesions usually have uniform light and dark pigment;
D. Diameter > 6 mm.

Melanoma and ionizing radiation

Cancers types which have been strongly correlated with exposure to ionizing radiation include thyroid cancer (exposure to radioactive iodine), leukemia (especially acute myeloid leukemia, AML), female breast cancer, and lung cancer. However, the relationship between ionizing radiation exposure and skin cancers in general/MM in particular remains unclear. Fink and Bates 2005 authored a review in response to concerns that ionizing radiation could be a cause of MM. This review was prompted by debate surrounding an observed excess of MM amoung empoyees of the Lawrence Livermore National Laboratory, a nuclear energy and weapons laboratory located in California (Fink and Bates 2005).

Studies presenting the relative risks for melanoma after ionizing radiation exposure fall in one of seven categories:

1. The Canadian Radiation Dose Registry;
2. Nuclear industy workers;
3. Subjects near nuclear test blasts;
4. Survivors of the atomic bombing in Japan;
5. Airline pilots and cabine attendants;
6. Recipiests of medical radiation;
7. Radiological technicians.

Gennerally, exposure categories with elevated relative risk of leukemia had proportionately elevated relative risks of MM (Fink and Bates 2005).

Pilots and airline crew are occupationally exposed to elevated levels of cosmic radiation, primarily neutrons and γ rays. Recent studies have found elevated SIRs (standardized incidence ratios) for well known radio-induced cancers, such as breast cancer, leukemia (especially AML), tumors of central nervous system, and multiple myeloma (Fink and Bates 2005). Studies are shown in Table 6.

Table 6 – Relative risk for MM and leukemia incidence in studies of aviation workers (Fink and Bates 2005)

Author, year	Description	Number of subjects	Melanoma		Leukemia	
			No.	SIR (95% CI)	No.	SIR (95% CI)
Band, 1990 (*27*)	Canadian commercial airline pilots	913	3	1.96 (0.49, 7.82)	2	Not reported
Pukkala, 1995 (*28*)	Finnish airline cabin attendants	1,577	3	2.11 (0.43, 6.15)	2	3.57 (0.43, 12.9)
Band, 1996 (*29*)	Canadian commercial pilots	2,740	8	1.52 (0.71, 3.26)	9	1.65 (0.80, 3.39)
Gundestrup, 1999 (*25*)	Danish commercial jet cockpit crew	3,790	7	2.5 (1.0, 5.2)	5	2.4 (0.8, 5.7)
Haldorsen, 2000 (*23*)	Norwegian airline pilots	3,701	22	1.8 (1.1, 2.7)	2	0.5 (0.1, 1.7)
Rafnsson, 2000 (*30*)	Icelandic commercial pilots	458	5	10.2 (3.29, 23.8)	1	1.69 (0.02, 9.43)
Haldorsen, 2001 (*24*)	Male Norwegian cabin attendants	588	6	2.9 (1.1, 6.4)	1	1.4 (0.0, 7.8)
Haldorsen, 2001 (*24*)	Female Norwegian cabin attendants	3,105	19	1.7 (1.01, 2.7)	1	0.6 (0.0, 3.4)
Reynolds, 2002 (*26*)	Female California flight attendants	49,118[a]	12	2.50 (1.28, 4.38)	0	—
Reynolds, 2002 (*26*)	Male California flight attendants	9,730[a]	3	3.93 (0.74, 11.6)	1	2.83 (0.0, 16.2)
Summary estimate				2.27 (1.96, 2.64)		1.64 (1.13, 2.38)
P for heterogeneity				0.94		0.80

[a] Calculated from data in paper.

The Canadian National Dose Registry and the Nuclear Industry workers group were the only two exposure categories where the risk of leukemia was generally not elevated, indicating that ionizing radiation exposure may have been lower than other categories. With the exception of these two categories the Fink and Bates review shows evidence for elevated relative risk for MM in every category of exposure to ionizing radiation examined, suggesting a relationship between ionizing radiation exposure and MM (Fink and Bates 2005).

Some investigators atribute the MM SIRs in airline crews to leisure time spent in tropical locations, resulting in increased exposure to UV radiation, rather than a direct effect of exposure of cosmic rays (Fink and Bates 2005). In-flight UV radiation exposure of pilots is not thought to be relevant, because cockpit windows provide considerable UV radiation protection (Haldorsen, Reiten and Tveten 2001). One study by Gundestrup and Storm, 1999, found higher incidence in jet pilots that in non-jet pilots, being jet crews more exposed to cosmic radiation than commercial crews. According to Gundestrup and Storm, the rate of cosmic radiation exposure can doble with every 1500m increase in altitude. (Gundestrup and Storm 1999)

Radiobiology

All living beings are constantly exposed to ionizing radiation. Environmental sources include cosmic radiation, earth radiation from inhaled and ingested materials. Air travels and mining activities increase background exposure. For instance, an air travel at 30 000 ft equals an equivalent dose of 0.5 mrem/h (5 µSv/h). Radiation originating from the body is mainly due to radioactive potassium, beta and gamma emitter. Lungs are exposed to radiation coming from inhaled air containing little amounts of radon. Cosmic radiation contributes with 280 µSv per year, while ground and internal sources with 260 and 270 µSv/year, respectively. Artificial sources mainly include medical related equipment, nuclear weapons and radioactive drugs. (Harrison's 2005)

Radiobiologic Interaction

Physical, chemical and biological phenomenon may occur when irradiating cells. Some tissues may be affected as consequence of cell damages, and then organs will be affected, spreading, finally, to whole body. This is a result of an interaction (energy transference) between radiation and the cells' atoms. The absorption of energy from radiation often leads to excitation or ionization. Excitation involves elevation of electrons to a higher energy state without actual ejection of the electron. Ion pairs are formed when interaction is sufficient to remove electrons from atoms: in this case we have what is called ionizing radiation. Ionizing radiation is subclassified as particulate and electromagnetic radiation (Table 7). Each photon has a quantized amount of energy given by Plank equation: E=hv, where *E* is the amount of energy in joules (J, SI unit) or, commonly used, electron-volt (eV), *h* is the Plank's constant ($6{,}626\,068\,96\times10^{-34}$ Js or $4{,}135\,667\,33\times10^{-15}$ eV) and v is radiation frequency in hertz (Hz = $1s^{-1}$).

Ionizing radiation may interact or not with irradiated tissues. Ionization occurs in three major ways:

- The photoelectric effect;
- The Compton effect;
- Pair production.

Photoelectric effect occurs at low energies (30 to 100 KeV). Here, the incident photon interacts with an electron from one of the outer shell of an atom (normally K, L or M) and ionization occurs if photon energy is greater than binding energy of the electron, in which case the electron is expelled from the orbit with a kinetic energy equal to the incident photon energy minus binding energy of the photon; upon returning to the initial shell, excited electrons emit non-ionizing electro-magnetic radiation, often UV radiation.

Table 7 - Common Types of Ionizing Radiation (modified from Harrison's 2005)

Type	Charge	Comment
Electromagnetic		
X-ray	0	X-rays and gamma rays only differ in the source. Gamma rays are produced by excited nucleus rearrangement, and x-rays are produced extranuclearly.
Gamma raw	0	
Particulate		
Electron	-1	β^- particle. May be accelerated close to speed of light. Quick deceleration and low penetration in tissues.
Positron	+1	β^+ particle. Similar to electron, when slowing interacts with electron producing 2 gamma photons with 511 KeV each.
Proton	+1	Mass about 2000 times of electron. Exhibits Bragg peak, means that proton beams exert their effect in a relatively compact region.
Neutron	0	Uncharged particle, impossible to accelerate by an EM field.
Alpha particle	+2	Helium nucleus: 2 protons + 2 neutrons. Very low tissue penetration.

Compton Effect occurs at higher energies, where incident photon interacts with an orbital electron not transferring all its energy. Part of the energy appears as kinetic energy of electrons and the residual energy continues as a less energetic deflected photon that may interact with another electron by Compton or photoelectric effect depending of its remaining energy.

Pair production only occurs when incident photon energy is greater than 1,024 MeV. In this case, photons interact with the nucleus producing an electron and a positron with the same kinetic energy, equal to the incident photon energy minus 1,024 MeV.

Physical phenomenons (atom ionization and the distribution of excitation energy throughout the cells) are the first to appear, followed by chemical phenomenons (free radical formation, due mainly to water radiolysis, and molecular bond breaking) and finally biological phenomenons that modify cell functions, morphology and normal activity, potentially leading

to cell death. These are the first reactions to ionizing radiation, generally occurring as a consequence of exposure to low doses. Main responsible for the cascade of events are the highly reactive free radicals, which lack a stable number of valence electrons. Cell damage is mainly due to hydroxyl radicals as follows:

$$h\nu + H_2O \rightarrow H_2O^+ + e^-$$

$$H_2O^+ + H_2O \rightarrow H_3O^+ + OH\cdot$$

$$OH\cdot \rightarrow \text{Cell damage}$$

Reactive oxygen species (ROS) are generated inside the cell as byproducts of the redox reactions in which oxygen is involved. A well known source of ROS is the utilization of oxygen in mitochondria during oxidative process of energy (ATP) and water production (Smit, et al. 2008).

According to modified Bergonie and Tribondeau law, cell susceptibility to ionizing radiation lesions is the same in different tissues, however, time of latency (period between irradiation and effect appearance) vary according to cell type and biological stress/effects will appear after cell division, making dividing cells (such as embryonary, epithelium, hematopoietic and tumor cells) more sensible to radiation-induced damage then mature slow or non-dividing cells (such as nervous cells). Consequently, different cells present different radio-sensitivity, so it is possible to classify living cells according to their division rate and radio-sensitivity: for instance, constant dividing hematopoietic cells are quite sensitive, in other hand, not so frequent dividing GI cells are less sensitive. Slow or non-dividing muscular and nervous cells are the least sensitive.

Cell rescue is a set of biological pathways involved in cell damage repair. Four important processes that occur after radiation exposure can be summarized as the “four R’s” of radiobiology:

Repair – repair of sublethal damage is temperature dependent and is thought to represent the enzymatic mechanisms responsible for intracellular injury healing;

Re-oxygenation – after radiation exposure in a tumor, oxygen and other nutrients are actually better distributed to viable cells;

Repopulation – cell population enhances cellular divisions in order to replace dying and dead cells;

Redistribution – the proportion of cells in different stages of the cell cycle is altered, due to the variability of cells’ radio-sensitivity over the cell cycle.

These mechanisms are responsible for reversing some of the radiation effects: in some cases cells are capable to repair some if not all damage, continuing to function normally. However, in some cases, the damage is too serious, leading to cell death; in this case, radiation must produce double-strand breaks in DNA. In other cases, however damaged, cells continue dividing; in this case, daughter cells may in turn die or also continue to divide without full

repair of the radiation lesion, perpetuating mutations which may lead to malignant tumor cell lines. Oxygen saturation is other important factor of sensitivity, as high levels of tissue and cellular oxygen increase the amount of reactive oxygen species produced.

Gray (Gy) is the SI unit of absorbed radiation dose and is defined as the amount of energy (Joules, J) absorbed by one kilogram (Kg) of matter; other important units are listed in Table 8. The main effects of radiation depend upon the absorbed dose and the length of exposure, therefore acute and chronic effects are defined.

Table 8 - Units and Definitions (Modified from (Harrison's 2005))

Unit	Quantity Measured	Definition
Roentgen (R)	Exposure	Amount of x-rays or gamma rays that produce 2×10^9 pairs of ions in 1 cm^3 of air at 0ºC.
Curie (Ci)	Radioactivity	Number of disintegrations per second in 1 g of ^{226}Ra.
Becquerel (Bq)	Radioactivity	Amount of disintegrations per unit of time in any radioactive specie. SI unit.
Rad	Dose	100 ergs deposited per gram of tissue or 0.01 J per kilogram of tissue.
Gray (Gy)	Dose	Amount of energy per unit of mass. (1 J/Kg). SI unit. 1 Gy = 100 rad.
Roentgen equivalent in men (Rem)	Dose equivalence	Reflects biologic response. Used to compare various types of radiation.
Sievert (Sv)	Dose equivalence	SI unit of dose equivalence; 1 Sv =100rem.

Acute and Chronic Effects

Acute effects occur by exposure to high doses of radiation in a small length of time, normally leading to a shortening of the life expectancy of the irradiated organism. Cell radio-sensitivity depends on the targeted organelle (nucleus, for instance, is more sensitive than cytoplasm) and the cell cycle phase (chromosome abnormalities typically occur in cells irradiated in the G1 phase; if cells are irradiated in the G2 phase, chromatid aberrations are more likely to result) and . Chromosomal abnormalities and mutations may lead to cell cycle alteration, cell death or malignant transformation. DNA radiation effects include base linkage alteration, base replacement (transversions or transitions); single and double strand breaks, which may induce mitosis inhibition or mitotic arrest, among other effects. Radiation-induced chromosomal modifications can be detected in metaphase.

When organisms suffer acute exposure, the clinical outcome can be classified in one of three radiation syndromes: Gastrointestinal (GI), Hematopoietic and Central Nervous System (CNS) syndrome. In the GI syndrome intestinal lumen cells lesions, dehydration, weight loss and serious infections may be present. In the Hematopoietic syndrome the most affected tissues are those responsible to blood cell production, causing anemia (erythrocytes loss) and

systemic infections (leukocytes loss). Efficiency of medical treatment increases when total doses are below 10 Gy.

Chronic effects occur in low dose exposures over long period of time. High doses tend to kill cells, damaging tissues and organs, while low doses tend to transform them: consequently, high doses usually trigger fast body response, while low doses interact at cellular level, and their results may be observed some time after cumulative exposure.

On chronic exposures we may also identify three types of effects: somatic effects, where only directly irradiated cells are affected, cancer being the major consequence; gonadal effects, where reproductive line cells are irradiated, potentially transmitting abnormalities to generations to follow; and *in-utero* effects, due to radiation exposure during gestation. In addition to these classical targeted effects of ionizing radiation, intense research activity has been focused recently on non-targeted IR effects, including genomic instability, adaptive response and bystander effects.

Radiation exposure increases the mutation rate, not the variety of types of mutations. Radio-induced cancers are similar in everything to spontaneous cancers, making it difficult to pin-point radiation as the underlying cause of a given cancer; however several large scale epidemiological studies have associated chronic radiation exposure to leukemia or thyroid, bone, lung, breast, skin cancers.

Radiation may also cause several fetus development damages: *in-utero* effects. Growing embryo is very sensible to radiation because it is made of very fast dividing cells with oxygen rich blood supply. *In-utero* death, congenital abnormalities, growth and development deficiencies and childhood cancers are major effects of *in-utero* exposure. Radiation damages depend upon fetus development stage. In terms of skin response to irradiation, an acute reaction can be seen after two weeks post exposure, and this latency can be correlated with the time required for cells to move from the basal to the keratinized layer of the skin. Skin reaction is characterized by erythema followed by dry desquamation and, sometimes, by edema. The vessels in the upper dermis are dilated and inflammatory infiltration is noted.

Chronic skin reaction can be seen starting 6 to 12 months after irradiation. Skin atrophy may occur resulting in higher sensitivity to injury than in normal skin. Interstitial fibrosis and telangiectasia (small dilated blood vessels near the surface of the skin or mucous membranes) may also be increased. Hyperpigmentation can be seen after a few months, fading gradually. The skin becomes thin and hair loss may be permanent. Radiation therapy can induce second malignancies, tending to be more aggressive than original cancers not related to radiation exposures.

Melanin

The group of compounds known as melanin comprises a class of tyrosine derivate compounds present in most living organisms, predominantly serving as high molecular weight pigments. Two most common forms of biological melanin are eumelanin and pheomelanin, considered to make up the mixed melanosomal melanin polymer present in human hair and skin. Microscopically, melanin is brown, non refractive and finely granular, with a diameter of less than 800 nm. Melanin is not soluble in water, but can be diluted in some organic solvents.

Types and Biosynthesis of Melanin

Eumelanin is a brown-black polymer of 5,6-dihydroxyindole (DHI), 5,6-dihidroxyindole-2-carboxylic acid (DHICA) monomer units, and their reduced forms. Pheomelanin is a red-brown polymer of benzothiazine. The higher number of electrons in oligomers of pheomelanin relative to eumelanin (Figure 9) – 388 versus 287 – could result in better scattering properties of pheomelanin (Dadachova E 2007). However, pheomelanin appears to provide a lower level of protection against UV radiation and, moreover, it is considered a possible source of free radicals when irradiated with UV (Smit, et al. 1998).

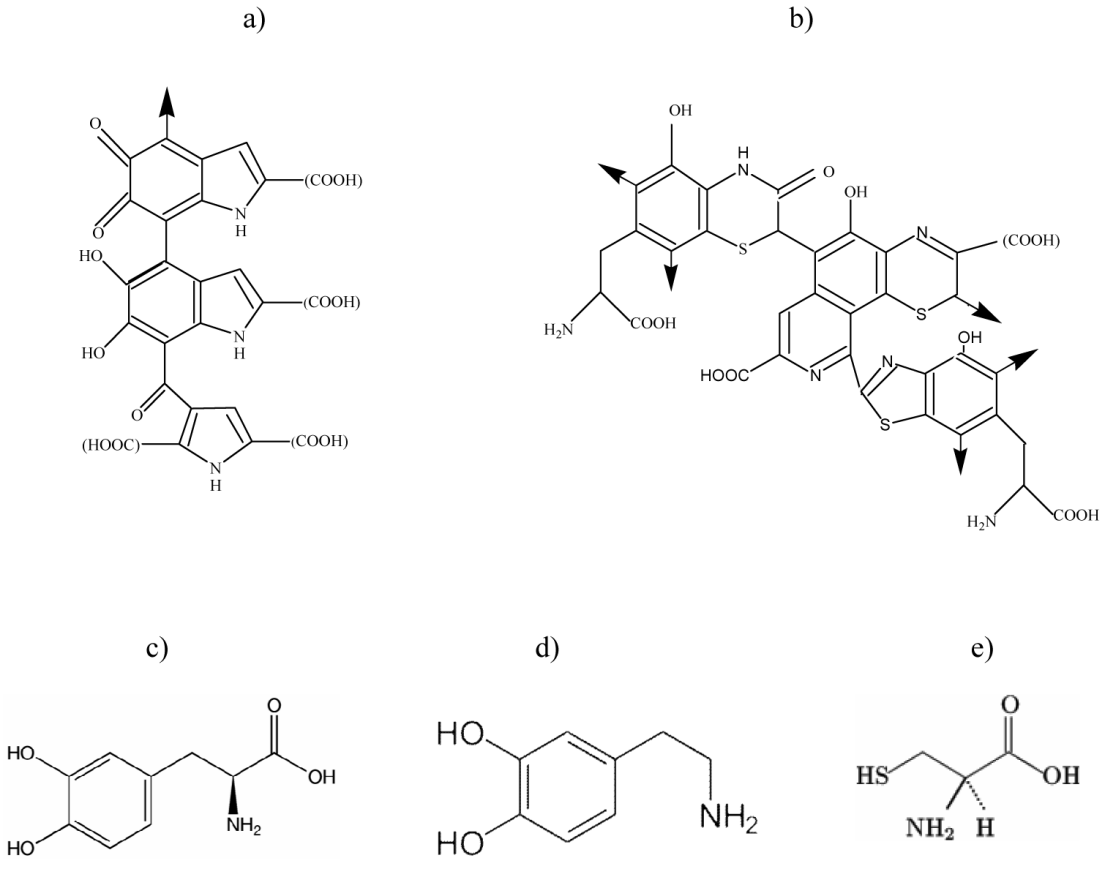

Fig. 9 – Chemical composition of melanin and its precursors: a) structure of eumelanin oligomer; b) structure of pheomelanin oligomer; c) L-Dopa; d) dopamine; e) L-tyrosine. (Howell, et al. 2008)

The first step of the biosynthetic pathway for both major types of melanin is catalysis by tyrosinase:

Tyrosine → DOPA → Dopaquinone

Dopaquinone can combine with cysteine by two pathways to produce benzothiazine and pheomelanin:

Dopaquinone + cysteine → 5-S-cysteinyldopa → benzothiazine intermediate → pheomelanin
Dopaquinone + cysteine → 2-S-cysteinyldopa → benzothiazine intermediate → pheomelanin

Dopaquinone can be converted to leucodopachrome and follow two more pathways to be converted to eumelanin:

Dopaquinone → leucopachrome → dopacrome → 5,6-dihidroxyindole-2-carboxylic acid → quinone → eumelanin
Dopaquinone → leucopachrome → dopacrome → 5,6-dihidroxyindole → quinone → eumelanin

At the secondary structural level there is no generally accepted model of melanin polymers with this uncertainty resulting from the multiple binding configurations that functionalized indoles can adopt. Two most prevalent models of melanin structure are: 1) heteropolymeric model which postulates that the melanin polymer forms via random bonding between monomers; 2) stacked oligomer model which suggests that melanins are composed of stacked oligomeric "proto-molecules" consisting of no more than 5–6 indolequinone units (Howell, Schweitzer, et al., Chemosorption of radiometals of ineterest to nuclear medicine by synthetic melanins 2008).

Melanogenesis

The increased production of melanin in human skin is called melanogenesis, usually taking place in UV stimulated melanocytes. The photochemical properties of melanin make it an excellent photo protector, absorbing harmful UV radiation and converting its energy into harmless amounts of heat through a process called “ultrafast internal conversion”. This property enables melanin to dissipate more than 99,9% of absorbed UV radiation as heat and keeps free-radical formation at minimum. The photoprotective properties of the pigment melanin and its precursors in cultured melanocytes or melanoma cells have been the subject of many studies (Smit, et al. 1998). Photoprotection by melanin is still a matter of investigation. The situation is complex because the composition as well as the quantity of the melanin in the skin is of importance for photoprotection or photosensitization. Elevated melanin production is connected to the risk of oxidative imbalance, may leading to mutations and provides a basis for malignant transformation of pigment cells (Smit, et al. 2008).

Hazardousness of melanin synthesis

As stated above, melanin is often considered to be a protective polymer because it absorbs UV radiation and scavenges diverse radicals. However, the production of this pigment involves oxygen-dependent generation of reactive ortho-dihydroxyindoles and –phenols and their respective (semi)quinones that polymerize with each other forming a polymer network (Smit, et al. 2008), and so melanin production is also considered as a potential (geno)toxic threat to melanocytes since different melanin precursors, formed during melanogenesis, exhibit high reactivity (ROS and other reactive molecules). Thus, the compartmentalization of melanogenesis by means of membrane-limited melanosomes has been postulated to be of great importance for the self-protection of cells (Smit, et al. 1998). However, Pheomelanin

synthesis consumes cysteine, limiting anti-oxidative defense. Recently it has been shown that these nevi synthesize more pheomelanin than do normal skin melanocytes (Smit, et al. 2008). As mentioned above, this metabolic disturbance can make them predisposed to oxidative stress.

Gamma Radiation Interaction with Melanin

The number of electrons per gram is an important contributor to the attenuation properties of a material at the energy levels where the Compton effect predominates (Dadachova E 2007). Compton scattering predominates for chemical elements with low atomic numbers such as C, N, O and S, which constitute melanin. In the Compton scattering, transfer of photon energy to matter occurs via a cascade of interactions, where the energy of the incident photon is transferred to high-energy electrons, and to secondary photons of progressively lower energy until the photoelectric effect takes place. Thus, the existence of structures composed of electron-rich, covalently linked aromatic motifs could explain the radiation scattering properties of melanins.

The high-energy electrons generated by Compton scattering are ultimately responsible for the biologic effects of gamma radiation by either direct interaction with DNA or through radiolysis of water in the cells, a process that results in the formation of reactive short-lived free radicals capable of damaging DNA. Melanin may interact with these high-energy electrons and prevent them from entering a cell, thus enabling its function as a radioprotector. The Compton electrons may then undergo secondary interactions with other melanin molecules, having their energy gradually lowered by melanin (Dadachova E 2007).

Protective role of melanin

Melanin is the primary determinant of human skin color and also found in hair, pigmented tissue underlying the iris, medulla and *zona reticularis* of the adrenal gland, *stria vascularis* of the inner ear and in pigmented-bearing neurons within areas of the brain stem, such as the *locus cereleus* and *substancia nigra pars compacta*. As previously stated, dermal melanin is produced by melanocytes, located in *stratum basale* of epidermis (Fig. 10). Melanocytes comprise from 5% to 10% of the cells in the basal layer of epidermis and are typically 7 µm in length. Although all human beings generally possess a similar amount of melanocytes in their skin (between 1000 and 2000 melanocytes per mm^2 of skin), the melanocytes in some individuals and ethnic groups more or less frequently express the melanin-producing genes, conferring greater or lesser concentration of skin melanin. *In vivo*, normal melanocytes transfer their melanosomes to keratinocytes lowering their own risk of oxidative stress (Smit, et al. 2008); melanin granules are transferred from melanocytes to keratinocytes in specialized vesicles called melanosomes. Melanosomes in each recipient keratinocyte cell accumulate atop the cell nucleus, protecting nuclear DNA. Molecular mechanism of melanin at cellular and sub-cellular level is not yet fully explained by biophysical and biochemical studies (Ghannam 2003).

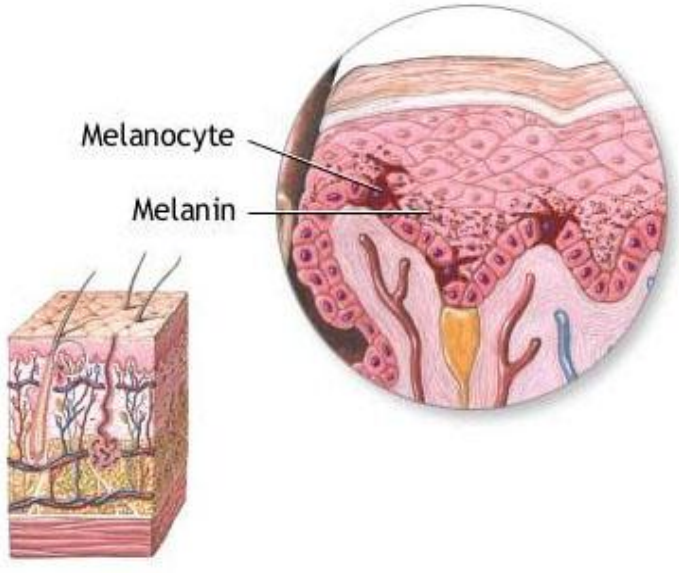

Fig. 10 - Skin structure and melanocyte localization in *stratum basale* of epidermis. (web-books.com 2009)

Melanins present numerous interesting physico-chemical characteristics including electromagnetic radiation absorption properties and the ability to chelate metals (Howell, et al. 2008). A recent study (Dadachova E 2007) showed evidences for radio-resistance in melanized fungi. These melanized fungal species colonize the walls of the highly radioactive reactor at Chernobyl and surrounding soils, often being dominant species in this kind of extreme environments and suggesting a role for melanin in radioprotection. In this work we hypothesized that an alteration in the melanin electronic properties alterations may occur due to radiation interactions that this may enhance the growth of melanized micro-organisms. Irradiated melanin manifests a 4-fold increase in its capacity to reduce NADH relative to non-irradiated melanin. It was found that also non-ionizing forms of radiation, infrared (IR), visible and UV light, increased the ability of melanin to transfer electrons, being independent of the energy of the incident photons (Table 9).

Table 9 - Increase in electron-transfer properties of melanin in NADH reduction after exposure to different forms of electromagnetic radiation (Dadachova E 2007)

Radiation Type	Photon energy, eV	Increase in initial velocity in NADH reduction
Ionizing radiation from ^{137}Cs source	661 000	4.0
UV, 254 nm	4.7	3.9
Visible light, 250 W	3	4.0
Heat, 348.15 K	0.1	3.7

To obtain additional evidence that exposure to ionizing radiation enhanced cell growth, Dadachova, *et al.* measured the incorporation of ^{14}C-labed acetate into melanized and non-melanized *C. neoformans* (fungi) cells with and without radiation flux. There was no incorporation of ^{14}C-acetate into heat killed melanized or non-melanized cells, which excludes the possibility that radiation promoted the passive absorption of ^{14}C-acetate on melanin. There was almost 3 times more incorporation of ^{14}C-acetate into irradiated melanized cells than into non-irradiated cells. These results demonstrate that the presence of melanin contributes to

the enhancement of cellular growth upon exposure to ionizing radiation in conditions of limited nutrients, because irradiated melanized cells experienced growth enhancement even in starvation conditions (Figure 11).

Radiation-induced effects on the electron-transfer properties of melanin were localized to the extracellular space thus establishing a spatial relationship between the site for electron-transfer events and the location of the melanin pigment. The ability to capture electromagnetic radiation and redox properties may confer melanized organisms with the ability to harness for metabolic energy (Dadachova E 2007).

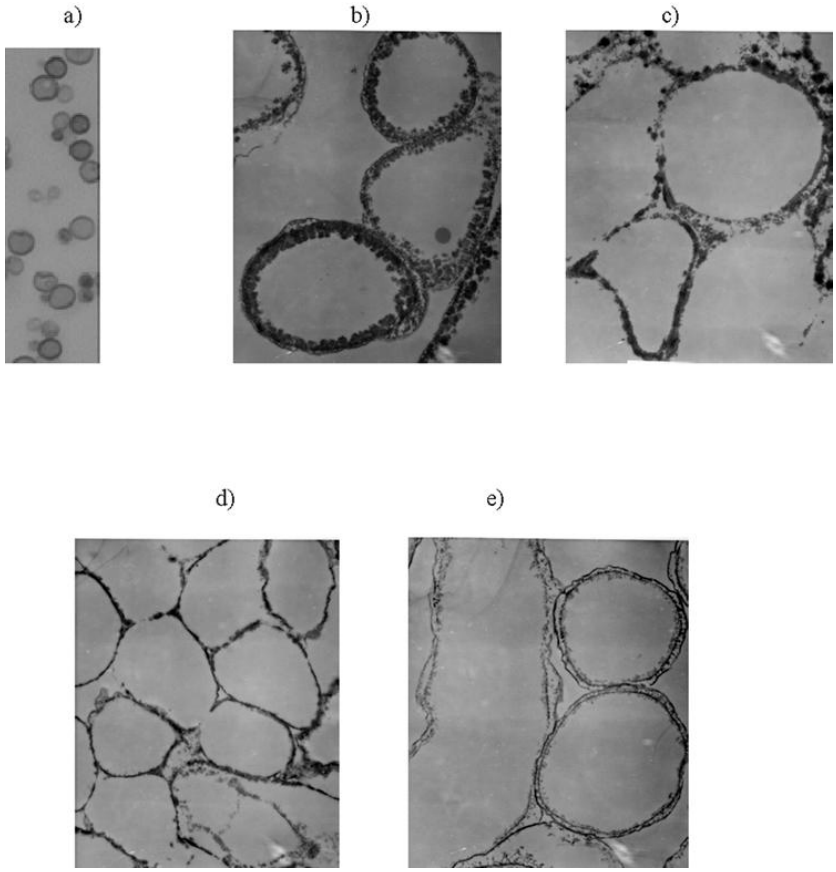

Fig. 11 - Microscopic images of melanized fungal cells: a) light microscopy image of C. neoformans melanin "ghosts"; (b–e) TEM images of C sphaerospermum "ghosts" derived from cells grown on nutrient rich or nutrient-deficient media: b) potato dextrose agar; c) Sabaroud dextrose agar; d) water agar with casein; e) water agar with dextrose. Original magnification: light microscopy image – X 1,000; TEM images – X 13,000 (Dadachova E 2007).

Recent research (Liu, et al. 2004) suggest that melanin is able to chelate metal ions through its carboxyle and phenolic hydroxyl groups, in many cases much more efficiently than ethylenediaminetetraacetate (EDTA). This hypothesis is supported by the fact that the loss of neuromelanin observed in Parkinson's disease is accompanied by an increase in iron levels in the brain. Howel *et al.* demonstrated that synthetic melanins made of diverse precursors can chemosorb ^{111}In, ^{213}Bi and ^{225}Ac radioactive metals with dopamine, L-dopa and tyrosine melanins being the most efficient. This property may be useful in bioremediation strategies whereby melanized microorganisms such as bacteria or fungi are potentially used to collect and immobilize heavy metals pollutants (Howell, et al. 2008).

These properties could also find an application in protecting bone marrow or gastrointestinal tract of cancer patients undergoing external beam radiation therapy (EBRT) or persons contaminated internally with radionuclides by administering melanin systemically in form of nanoparticles or powders. The advantage of synthetic melanin over other radioprotectors or metal chelating agents is its complete chemical inertness (Howell, et al. 2008).

In vitro melanin production

Smit, *et al.* 1998, performed an evaluation of the influence of different culture media on pigment production. With higher L-tyrosine concentrations in the medium, pheomelanogenesis as well as increased eumelanin synthesis were stimulated in all cultures tested. This stimulation was particularly prominent in type I (pale white skin, blue/hazel eyes, blond/red hair individuals) skin melanocytes than type IV (light brown skin individuals) skin melanocytes.

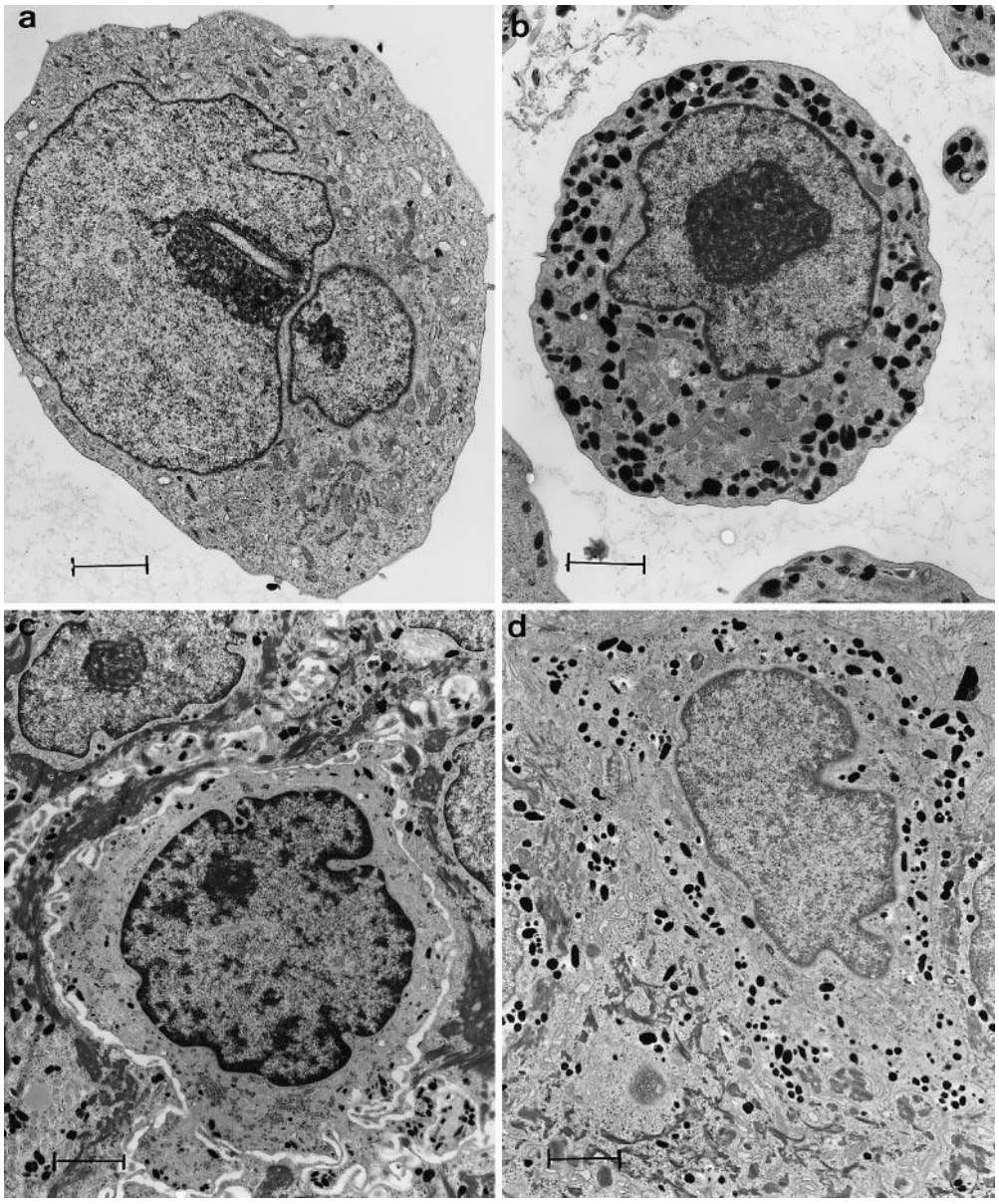

Fig. 12 - TEM showing the microscopic pigmentations phenotypes of melanocytes: a) skin type I *in vitro* (bar 1.15 µm); b) skin type IV *in vitro* (bar 0.17 µm); c) skin type I *in vivo* (bar 0.17 µm); d) skin type VI *in vivo* (bar 0.12 µm) (Smit, et al. 1998).

Cell Line and Culture

Cell Line

B16-F1 mouse melanoma cells, with melanin producing capability, were used in this work. This cell line has an adherent growth pattern and fibroblast-like morphology (Fig. 13 left).

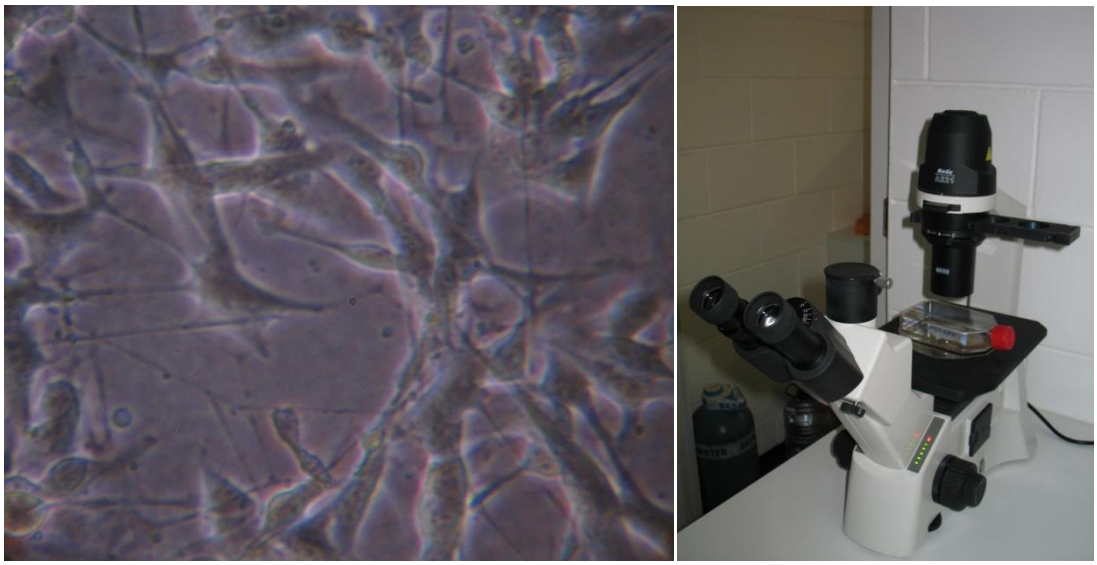

Fig. 13 - B16-F1 cell culture (left) – image acquired with Motic AE21 inverted microscope (400X) (right) and Cannon Powershot A620 Digital Camera

Culture medium

The base medium for cell growth was Dulbecco's Modified Eagle's Medium with L-glutamine (DMEM D5648, Sigma Aldrich, St. Louis, MO) supplemented with 10% Foetal Bovine Serum (FBS) and 1% antibiotics (penicillin and streptomycin).

Cell culture and subculture routine

The cell culture was conducted in T75 CellStar® Greiner Bio-One culture flasks, with subculture density of 1 ml cell suspension to 9 ml of supplemented DMEM medium (10 ml total volume), kept at 37°C temperature, 5% carbon dioxide humidified atmosphere. When 70 – 80% confluence was reached subcultures where performed by removing medium, washing with phosphate-buffered saline (PBS), adding 1 ml trypsin-EDTA solution (0.25% trypsin, 0.53 mM EDTA), after which the cells were allowed to detach by sitting the flask sits at 37°C for a few minutes, followed by adding 9 ml of fresh culture medium with FBS (which contains trypsin inhibitors). 1 ml of the cell suspension was dispensed into a new culture flask (as detailed above) and medium was renewed every 3 days.

Irradiation Equipment

The irradiation equipment, a high activity gamma AECL ELDORADO 6 irradiator (^{60}Co 92.5 TBq source) (Fig. 14), was part of the Metrological Laboratory of Ionizing Radiation and Radioactivity of the Technological and Nuclear Institute.

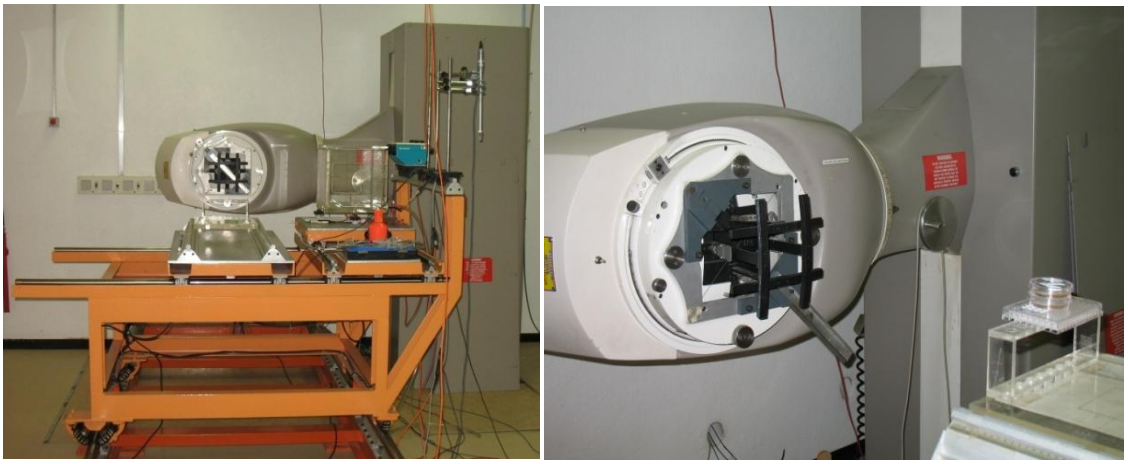

Fig. 14 - AECL ELDORADO 6 Irradiator high activity ^{60}Co 92.5 TBq source.

For the irradiation procedure a 10x10 cm field at 1 m from the source was used (Fig. 14 right). The dose rate at this distance was 0.1099 Gy/min. For example, for an exposure dose of 1.5 Gy, the length of irradiation was 13.65 min (Fig. 15 left).

Fig. 15 - Left: Irradiator command unit. Right: Environmental dose equivalent monitor performs readings inside irradiation bunker.

Biomarkers for Genotoxicity (CBMN assay)

The *in vitro* cytokinesis-blocked micronucleus assay (CBMN assay) is a genotoxicity test system based on the detection of micronuclei (MNi), small inclusions of DNA material, in the cytoplasm of interphase cells. These MNi may originate from acentric fragments or whole chromosomes that are unable to migrate with the remaining chromosomes during the anaphase of mitosis due to structural alterations caused by exposure to mutagenic and genotoxic physical and chemical agents (OECD 2006). At telophase, a nuclear envelope forms around chromosomes and fragments, which then uncoil and gradually assume the morphology of an interphase nucleus with the exception that they are smaller, hence the term “micronucleus” (Fenech 2000).

The micronucleus assay has emerged as one of the preferred methods for assessing chromosome damage because it allows for the reliable detection of both aneuploidy (chromosome loss) and chromosome or chromatid breakage. Because MNi are only expressed in cells that complete one nuclear division after damage, a special method was developed that identifies recently divided cells by their binucleated (BN) appearance when blocked from performing cytokinesis using cytochalasin-B (Cyt-B), a microfilament-assembly inhibitor. The CBMN assay presents a good reproducibility, as the results obtained are not biased by potentially altered division kinetics caused by direct cytotoxicity of the agents tested or by sub-optimal cell culture conditions. The method is now applied for specific purposes in radiobiology, such as the prediction of the radiosensitivity of tumors and the inter-individual variation in radiosensitivity (Fenech 2000).

The CBMN assay has a number of advantages over metaphase analysis used to score chromosomes aberrations, as described in the OECD Guidelines 473 and 475 (OECD 2006). Because MNi in interphase cells can be assessed more objectively than chromosomal aberrations in metaphase cells, a less detailed training is required for testing personnel to achieve competence. In the CBMN there is no need to count the chromosomes as in metaphase preparations, but only to determine whether or not the cells contain micronucleus. As a result, there is a significant increase in throughput of scoring, with positive impact in the statistical power of the study, given that thousands instead of hundreds of cells can be scored per treatment (OECD 2006).

Chromosome breaks may arise from unrepaired double strand breaks in DNA. It is also recognized that chromosome partial or total loss, aneuploidy and non-disjunction are important events in cancer and they are probably caused by defects in the spindle, centromere or as a consequence of under-condensation of chromosome structure before metaphase (Fenech 2000). Therefore, the mechanism that causes the increased frequency of MNi is directly implicated in the carcinogenic pathway.

Because MNi are only expressed in cells that have completed nuclear division, they are ideally scored in the BN stage of the cell cycle. Occasionally nucleoplasmic bridges between nuclei in BN cell are observed. These are probably dicentric chromosomes in which the two

centromeres were pulled to opposite poles of the cell and the DNA in the resulting bridge covered by nuclear membrane (Fig 16) (Fenech 2000).

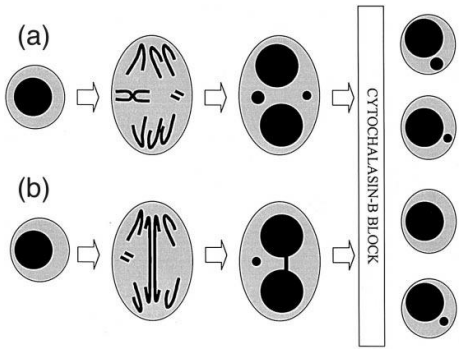

Fig. 16 a) - The origin of MNi from lagging whole chromosomes and acentric fragments during anaphase. b) - The formation of nucleoplasmic bridge from a dicentric chromosome. The critical role of Cyt-B in blocking dividing cells at the BN stage is also indicated in this diagram (Fenech 2000).

The method was initially developed for use with cultured human lymphocytes, but has now been adapted to various cell types such as solid tumors. The most critical points of the method are:

a) Analyzing exclusively BN cells to ensure that MNi are scored in the first nuclear division following the irradiation;
b) Allowing sufficient time for Cyt-B to act: it takes up to 6h before it starts to exert its cytokinesis-blocking action.

Criteria for selecting BN cells which can be scored for MNi frequency

The cells that may be scored for MNi frequency should have the following characteristics (Fenech 2000):

a) The cells should be BN;
b) The two nuclei in a BN cell should have intact nuclear membranes and be situated within the same cytoplasmic boundary;
c) The two nuclei in a BN cell should be approximately equal in size, staining pattern and intensity;
d) The two nuclei within a BN cell may touch, but ideally should not overlap each other. A cell with two overlapping nuclei can be scored only if the nuclear boundaries of each nucleus are distinguishable;
e) The two nuclei within a BN cell may be attached by a fine nucleoplasmic bridge which is no wider than $1/4^{th}$ of the nuclear diameter;
f) The cytoplasmic boundary or membrane of a BN cell should be intact and clearly distinguishable from the cytoplasmic boundary of adjacent cells.

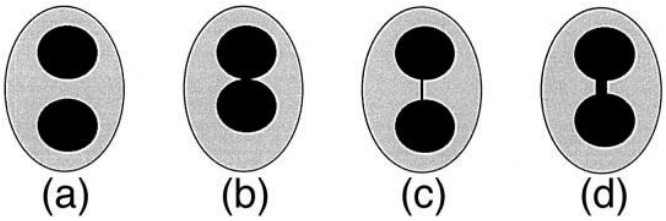

Fig. 17 a) ideal BN cell; b) BN cell with touching nuclei; c) and d) BN cells with nucleoplasmic bridge (Fenech 2000).

Examples of the type of BN cells that may be scored are illustrated in Fig. 17. The cell types that **should not** be scored for MNi frequency include mono-, tri-, tetra- and multi-nucleated cells, and cells that are apoptotic or necrotic (Fig. 18)

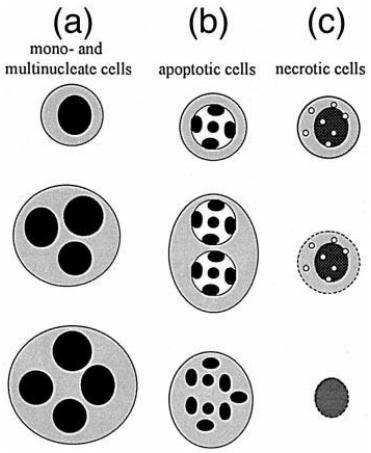

Fig. 18 - The various types of cells that may be observed in the *in vitro* CBMN assay excluding BN cells. These cell types should not be scored for MNi frequency (Fenech 2000).

Criteria for scoring MNi

MNi are morphologically identical to, but smaller than, nuclei. They also have the following characteristics (Fenech 2000):

a) The diameter of MNi usually varies between 1/16th and 1/3rd the mean diameter of the main nuclei which corresponds to 1/256th and 1/9th the area of one of one of the main nuclei in a BN cell, respectively;
b) MNi are non-refractive and they can therefore be readily distinguished from artifacts such as particles of staining reagent;
c) MNi are not linked or connected to the main nuclei;
d) MNi may touch but not overlap the main nuclei and the micronuclear boundary should be distinguishable from the nuclear boundary;
e) MNi usually have the same staining intensity as the main nuclei but occasionally staining may be more intense.

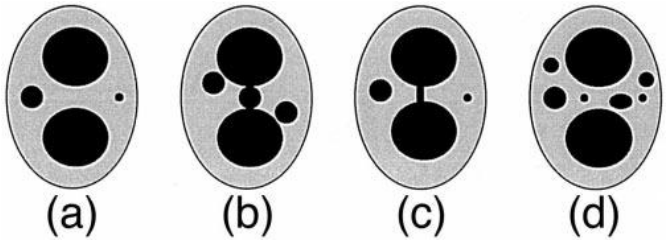

Fig. 19 a) Cell with two MNi, one with 1/3rd and the other 1/9th the diameter of one of the main nuclei within the cell; b) MNi touching but not overlapping the main nuclei; c) A BN cell with nucleoplasmic bridge between the two main nuclei and two MNi; d) A BN cell with six MNi of various sizes (Fenech 2000).

Examples of typical MNi that meet the criteria set above are shown in Fig. 19. Examples of cellular structures that resemble MNi but should not be classified as MNi originating from chromosome breakage or loss are illustrated in Fig. 20.

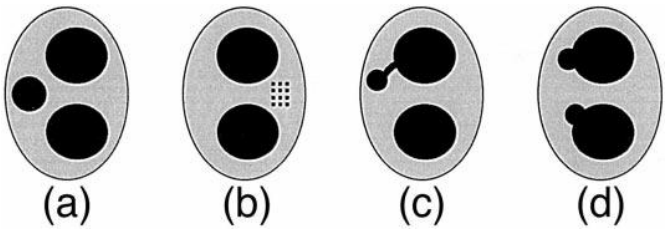

Fig. 20 Occasionally BN cells (or cells that resemble BN cells) may contain structures that resemble MNi but should not be scored as MNi originating from chromosome loss or chromosome breakage. These situation include: a) a trinucleated cell in which one nucleus is relatively small but has a diameter greater than 1/3 the diameter of the other nuclei; b) dense stippling in a specific region of cytoplasm; c) extruded nuclear material that appears like a MNi with a narrow nucleoplasmic connection to the main nucleus and d) nuclear blebs that have an obvious nucleoplasmic connection with the main nucleus (Fenech 2000).

Procedures and Results

B16-F1 cells were subcultured in 5 cm diameter sterile Petri dish ($1x10^5$ cells each) 24h before irradiation procedure. At 44 h of incubation, cytochalasin-B was added to the culture medium. At the end of incubation, cells were harvested by trypsinization, centrifuged, washed with washing solution twice and submitted to a mild hypotonic shock to enlarge the cytoplasm of the cell and improve scoring. The cells are then smeared onto clean glass slides, allowed to dry, fixed, and stained by Giemsa (complete protocol in Appendix 2, Protocol 1). All calculations were performed using Microsoft™ Excel 2007 or manually. Slides were scored in an optical transmitted light Carl-Zeiss D-7082 Oberkochen microscope, slide scanning at 250X magnification and MNi confirmation at 400X magnification.

For choosing a gamma radiation dose, dose-response screening experiments were performed at 0, 0.5, 1, and 2 Gy. Results are listed in Table 10 and depicted in Fig. 21 chart.

After analysis of the results, an interpolated irradiation dose of 1.5 Gy was chosen to obtain an adequate significance for the different melanin concentration assays.

Table 10 – CBMN assay micronuclei frequency at 0, 0.5, 1.0 and 2.0 Gy

Dose (Gy)	Mono-micronucleated cells		Poly-micronucleated cells		Total micronucleated cells	
	Mean	SD	Mean	SD	Mean	SD
0.0	2,000	1,414	0,000	0,000	2,000	1,414
0.5	12,000	0,000	2,000	0,000	14,000	0,000
1.0	15,667	7,095	1,667	0,577	17,333	6,658
2.0	51,000	15,556	12,500	0,707	63,500	14,849

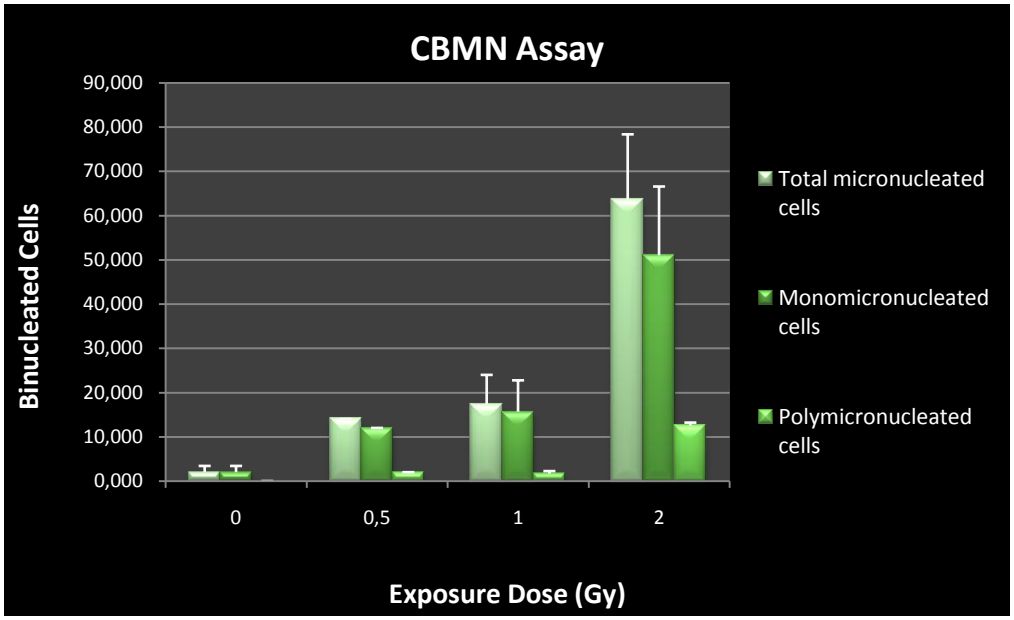

Fig. 21 – CBMN assay micronuclei frequency at 0, 0.5, 1 and 2 Gy chart.

Because melanin is insoluble in water, a 10 g/l melanin-DMSO solution was made. In early experiments, higher concentrations of melanin were also tested, however a solubilisation problem was verified when the melanin-DMSO solution was added to the cells and so melanin was kept at stably soluble levels in the final media.

Different synthetic melanin (Sigma-Aldrich, St Louis USA) concentrations added to the cell culture were irradiated at 1.5 Gy Non-irradiated cells were used as control. Results of MNi quantification after irradiation in the presence of different melanin concentrations are listed in Table 11 and depicted in Fig. 22 chart.

Table 11 – CBMN assay micronuclei frequency in B16-F1 cells irradiated at 1.5Gy of gamma radiation in the presence of different concentrations of melanin added in medium. Non-irradiated cells were used as control.

Melanin Concentration g/l	Monomicronucleated cells		Polimicronucleated cells		Total micronucleated cells	
	Mean	SD	Mean	SD	Mean	SD
Control cells	2,00	1,41	0,00	0,00	2,00	1,41
0,02	99,00	8,75	23,60	5,22	122,60	11,30
0,10	85,50	5,45	18,25	2,87	103,75	7,80
0,20	61,80	13,77	11,40	3,91	73,20	17,47

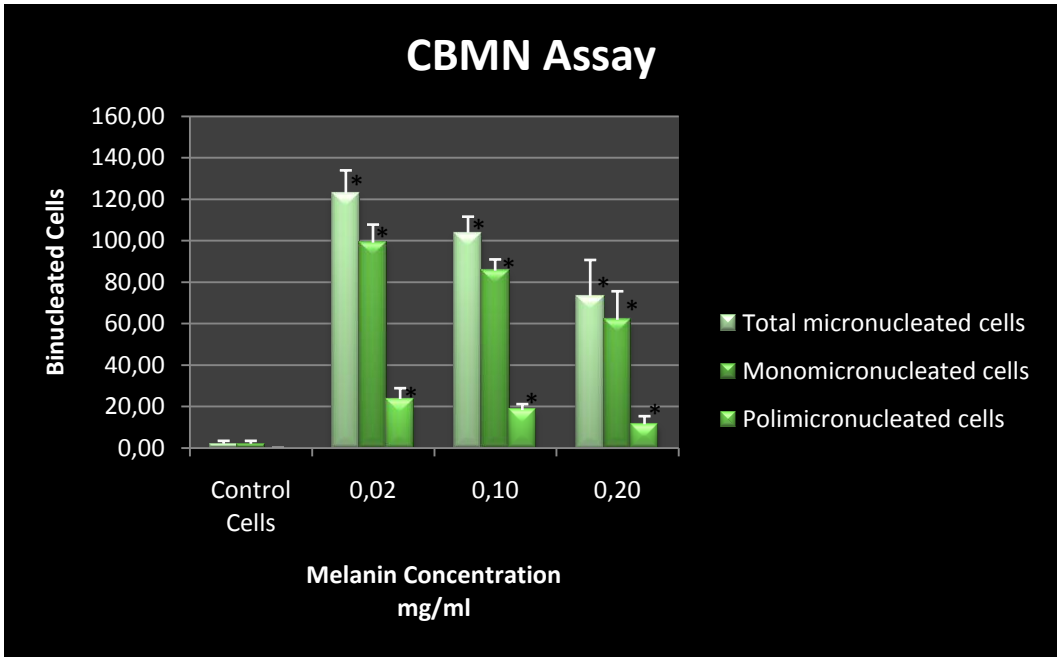

Fig. 22 - CBMN assay micronuclei frequency in B16-F1 cells irradiated at 1.5Gy of gamma radiation in the presence of different concentrations of melanin added in medium; non-irradiated cells were used as control(*) $p<0.05$ between different melanin concentrations and compared to control (Student's t-test).

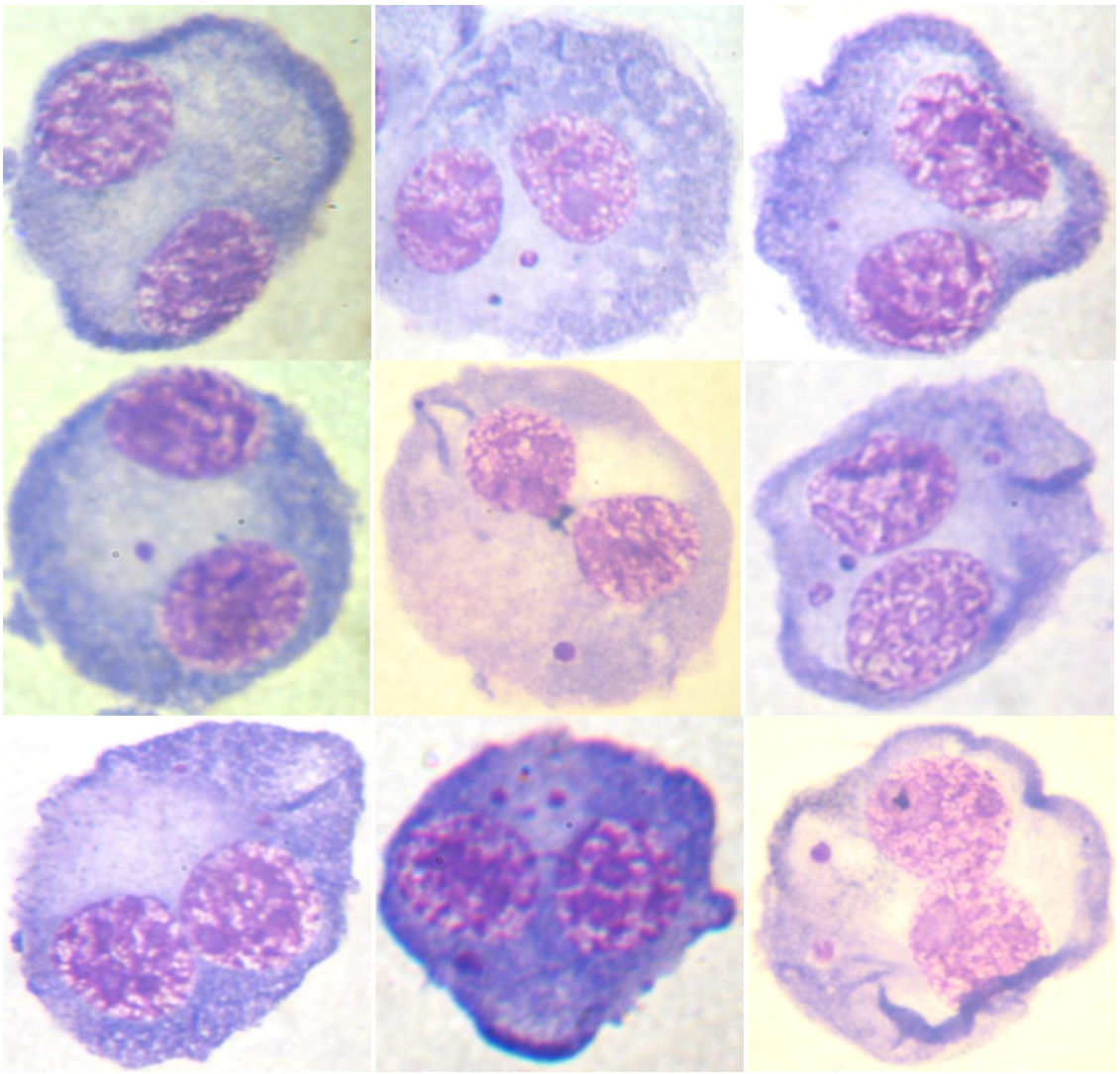

Fig. 23 - Examples of binucleated (BN) cells observed in the slides. Top left – BN cell without micronuclei (MNi). Top center, top right, middle left and middle center – BN cells with one MNi. Middle right and bottom – BN cells with more than one MNi. Images obtained using an optical transmitted light Carl-Zeiss D-7082 Oberkochen microscope (400x magnification) and Canon Powershot A620 digital camera.

Acute Cytotoxicity – MTT Assay

This method is a simple quantitative assay to determine the cellular viability in samples, by analyzing the capacity of cells to metabolize MTT in a mitochondria-dependent reaction, producing a colored compound, formazan, to which the cell membrane is impermeable.

The tetrazolium salt 3-(4,5-dimethylthiazol-2-yl)-2,5-diphenyltetrazolium bromide (MTT) is taken into cells and reduced by mitochondrial succinic dehydrogenase activity to yield a purple formazan product (Ibelgaufts 2008). Chemical structures of substrate and final compound are presented in Fig. 24. The product accumulates within the cell, due to the fact that it cannot pass through the plasma membrane. Upon cell membrane disruption by organic solvents, the product is released and can be readily detected and quantified in the supernatant by a UV/Visible spectrophotometry.

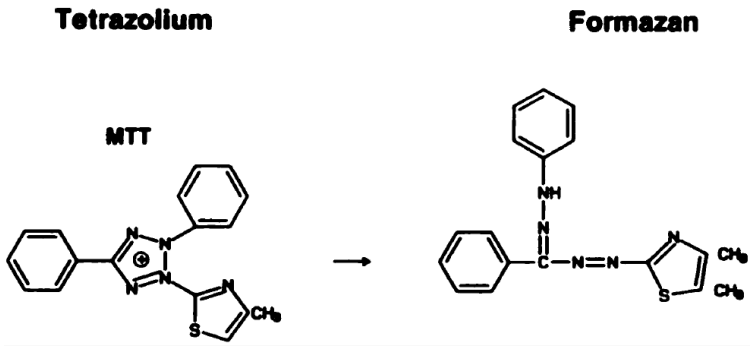

Fig. 24 – Structures of MTT tetrazolium and formazan (Scudiero, et al. 1988).

The ability of cells to reduce MTT provides an indication of mitochondrial integrity and activity which, in turn, may be interpreted as measure of viability and/or cell proliferation. Determination of cellular ability to reduce MTT to formazan after exposure to a toxic aggression, when compared to control samples provides a measure of the relative toxicity experienced by the cells under exposure conditions (Mosmann 1983).

Procedure and Results

Cultured B16-F1 cells were plated into 96-well flat bottom microplates with different synthetic melanin (Sigma-Aldrich, St Louis USA) concentrations added to the media, incubated for 24 h and irradiated at 1.5 Gy exposure dose. 24h post-irradiation the cells were exposed to MTT during 4h, after which 200µL of DMSO were added to each well to disrupt cell membranes and extract the formazan into the supernatant. The amount of solubilized formazan product in each well was determined using a Rosys Anthos 2010 microplate reader spectrophotometer (Fig 25), with readings performed at 540 nm and using 620 nm as reference wavelength (see complete protocol in Appendix 2, Protocol 2). The amount of formazan present in exposed samples conditions was expressed as a percentage of that occurring in the control samples, as follows:

$$\%\ cell\ survival = \frac{absorbance\ of\ treated\ cells}{absorbance\ of\ control\ cells} \times 100\ \%$$

Uncertainty of measurement was calculated using uncertainty propagation method (see appendix 1: data analysis – uncertainty propagation) which gave the expression:

$$\sigma_{cs}^2 = \left(\frac{1}{absorbance\ of\ control\ cells}\right)^2 \sigma_A^2$$

Where σ_{cs}^2 is the variance in cell survival and σ_A^2 is the variance in absorbance measurements. All calculations were performed using Microsoft™ Excel 2007 and/or manual methods.

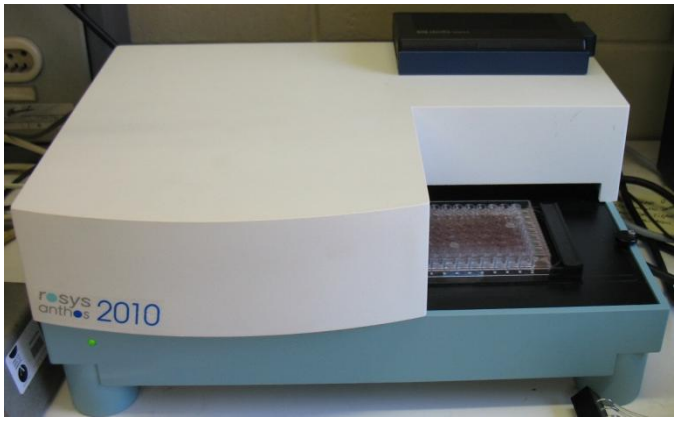

Fig. 25 - Rosys Anthos 2010 microplate reader spectrophotometer.

Results at different melanin concentration are listed in Table 12 and depicted in Fig. 26 chart.

Table 12 – MTT assay results in B16-F1 cells irradiated at 1.5Gy of gamma radiation in the presence of different concentrations of melanin added in medium. σ_A is the standard deviation in absorbance measurements and σ_{cs} is the standard deviation in cell survival.

Doses	0 Gy	1,5 Gy				
Melanin Concentration (mg/ml)	0	0	0,1	0,15	0,2	0,5
Absorbance Mean	0,247	0,177	0,224	0,294	0,357	0,482
σ_A	0,038	0,023	0,047	0,071	0,050	0,043
% Cell Survival	100%	72%	91%	119%	145%	195%
σ_{CS}	16%	9%	19%	29%	20%	17%

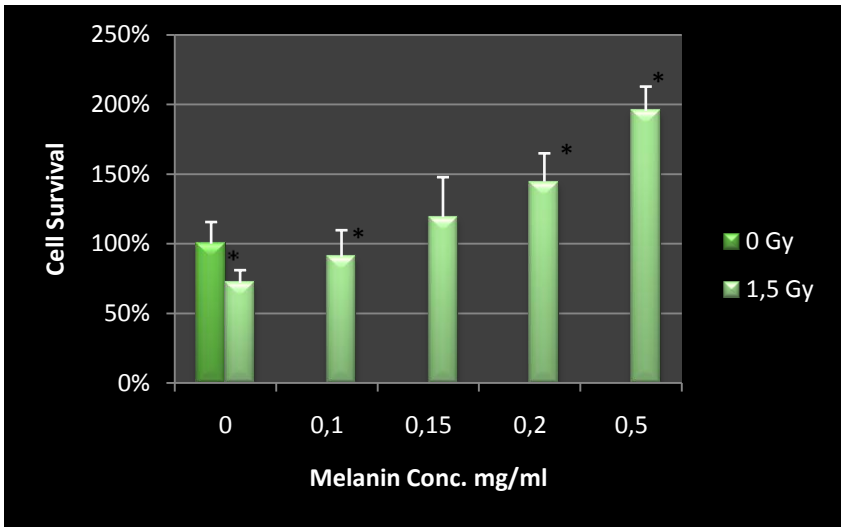

Fig. 26 – MTT cell survival results in B16-F1 cells irradiated at 1.5Gy of gamma radiation in the presence of different concentrations of melanin added in medium. (*) p<0.05 compared to control (Student's t-test).

The previous experiments were focused on the effects of extracellular melanin concentration in radiation damage. In order to investigate the pattern of melanin modulation of radiation damage with different intracellular concentrations of melanin B16-F1 cells were incubated in Ham F10 media (Sigma-Aldrich, St Louis USA), with low and high concentration of melanin precursor, tyrosine. Hams F-10 medium was chosen for its low L-tyrosine content. Final concentrations used were the following: 0.01 mM concentration of L-tyrosine (1T- 0.01 mM tyrosine in the original Ham´s F-10 medium) and 40 times that concentration of L-tyrosine (40T – 0.4 mM) as described by Smit, et al. 1998. Results of MNi assay after 1.5Gy irradiation in cells grown in the different melanin concentrations are listed in Table 13 and depicted in Fig. 27 chart.

Table 13 - MTT assay results in B16-F1 cells irradiated at 1.5Gy of gamma radiation for 1T and 40T L-tyrosine concentrations in culture medium. σ_A is the standard deviation in absorbance measurements and σ_{cs} is the standard deviation in cell survival.

Dose	0 Gy	1,5 Gy	
Culture Media	**1T**	**1T**	**40T**
Absorbance Mean	0,259	0,224	0,228
σ_A	0,047	0,049	0,048
% Cell Survival	100%	86%	88%
σ_{CS}	18%	19%	19%

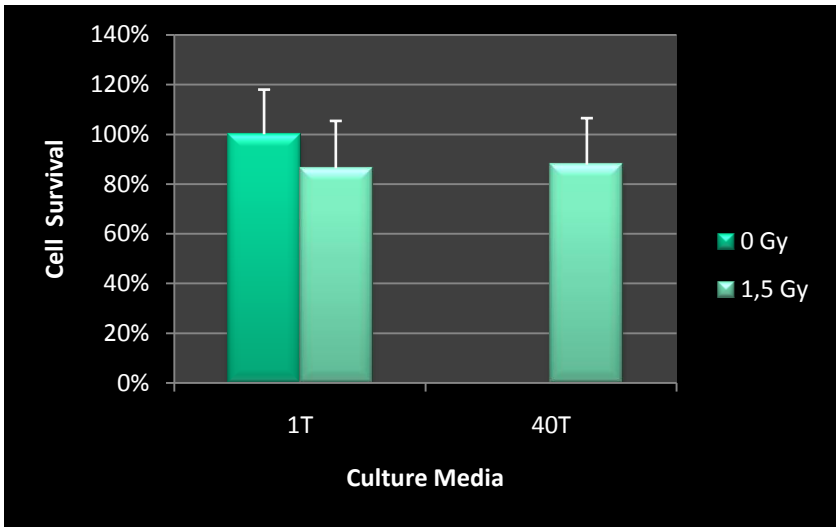

Fig. 27 - MTT assay results in B16-F1 cells irradiated at 1.5Gy of gamma radiation for 1T and 40T L-tyrosine concentrations in culture medium. No statistical significant differences were found between the groups.

Oxidative Stress determination – MDA quantification

Oxidative stress generates reactive oxygen species (ROS) that can interact with phospholipids and fatty acids to generate many reactive products including aldehydes. This process is commonly referred to as lipid peroxydation. Of the many biological targets of oxidative stress, lipids are the most involved class of biomolecules. Lipid peroxydation gives rise to a number of secondary products, which perpetuate the cascade of oxidative These products are mainly aldehydes, with the ability to exacerbate oxidative damage due to the longevity and high reactivity of these molecules, allowing them to act inside and outside the cells, interacting with critical biomolecules such as nucleic acids and proteins, often irreversibly damaging the delicate mechanisms in cell functionality (Del Rio, Stewart and Pellegrini 2005). Although lipid peroxidation occurs under normal physiological conditions, it becomes significant during viral and bacterial infection, xenobiotic and radiation exposure, and inflammation (Feng, et al. 2006).

Malondialdehyde (MDA) is a major product of lipid peroxidation, being the principal and most studied product of polyunsaturated fatty acid peroxidation (Del Rio, Stewart and Pellegrini 2005); it not only reacts with cellular nucleophiles but also leads to self condensation to form MDA oligomers (Marnett 2002). MDA first shown to be carcinogenic in 1972 following topical administration to mice. This was an unusual result because the tumors arouse in a very short time and were not the type of tumors typically seen in a mouse skin assay (Marnett 1999). Most assays to determine MDA have been developed on the basis of its derivatization with thiobarbituric acid (TBA). The condensation of these two molecules gives rinse to form a complex that can be quantified by spectrophotometry and fluorimetry (Del Rio, Stewart and Pellegrini 2005). Nevertheless, this reaction is not specific of MDA, since other compounds (other aldehydes, bilirubin) can react with thiobarbituric acid, and other chromophores present in the biological samples may absorb or fluoresce in the same wavelengths as the MDA-TBA complex. In an attempt to overcome this limitation, the TBA-MDA complex is extracted from the reaction mixture with an organic solvent, and the quantification is made using this extract (Goulart de Medeiros 2003).

Procedures and Results

Quantification of TBA reactive substances was based on the technique described by Dousset *et al.* (1983), with modifications. TBA reagent was added to triplicate samples of post-irradiation (2-3 hours after irradiation) cell supernatant and heated at 100ºC for 10 minutes in order to favor the formation of the complex. Butilhydroxytoluene (BHT) was added to the reaction medium to avoid oxidation of lipids in the sample and the production of MDA artifacts during the 100ºC incubation. The complex was extracted from the aqueous phase by a fixed volume of 1-butanol, and the fluorescence of the organic solution was measured. A calibration curve was prepared using tetramethoxipropane (Fluka AG, Buchs Switzerland), which hydrolyses to MDA in water (see detailed protocol in Appendix 2, Protocol 3) (Goulart de Medeiros 2003). For fluorimetry measurements a Shimadzo RF-5000 spectrofluorophotometer

was used (Fig. 28). All calculations were performed using Microsoft™ Excel 2007 and manual methods.

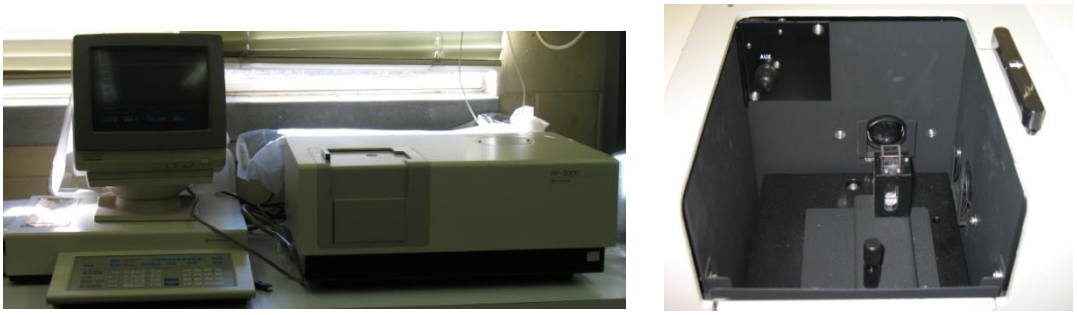

Fig. 28 – Shimadzo RF-5000 spectrofluorophotometer.

In the first set of experiments, different synthetic melanin concentrations in media were used. Calibration curve results are listed in Table 14 and depicted in Fig. 29 chart. From these results a function was obtained by linear least square fitting method (see appendix 1: data analysis – linear least square fitting method), where fl corresponds to fluorescence and sc to standard concentration, σ_a is the uncertainty of parameter a and σ_b the uncertainty of parameter$b$. The function obtained was inverted to obtain concentration in function of fluorescence. Uncertainty of measurement was calculated using the uncertainty propagation method (see appendix 1: data analysis – uncertainty propagation). MDA assay results for the different concentrations of added melanin are listed in Table 15 and depicted in Fig. 30 chart.

Table 14 – Calibration curve results - MDA assay for different concentrations of melanin. SD is the standard deviation.

Standard concentration (10^{-6} mol/ml)	Mean	SD
0,00	4,594	0,219
0,25	24,140	1,552
0,50	43,533	1,790
1,50	118,932	1,453
2,50	195,000	2,928

$$fl = 4.611 + 76.285sc$$

$$\sigma_a = 0.217$$

$$\sigma_b = 0.740$$

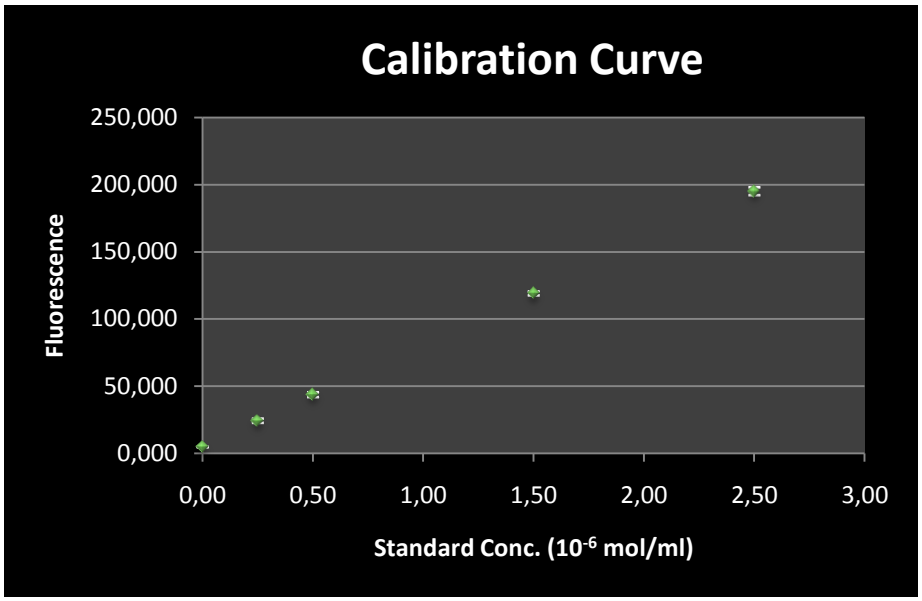

Fig. 29 - Calibration curve results - MDA assay for different concentrations of melanin.

$$sc = \frac{fl - 4.611}{76.285}$$

$$\sigma_{sc}^2 = \left(\frac{\partial sc}{\partial fl}\right)^2 \sigma_{fl}^2 = \left(\frac{1}{76.285}\right)^2 \sigma_{fl}^2$$

Table 15 – MDA assay results in B16-F1 cells irradiated at 1.5Gy of gamma radiation for different concentrations of melanin added in culture medium. σ_{SC} is the standard deviation in standard concentration.

Dose	Melanin Concentration (mg/ml)	Standard Concentration (10^{-8} mol/ml)	σ_{sc}
0 Gy	**0,00**	24,457	1,400
1.5 Gy	**0,00**	28,008	1,037
	0,02	26,075	0,853
	0,10	25,124	0,725
	0,20	24,651	0,813

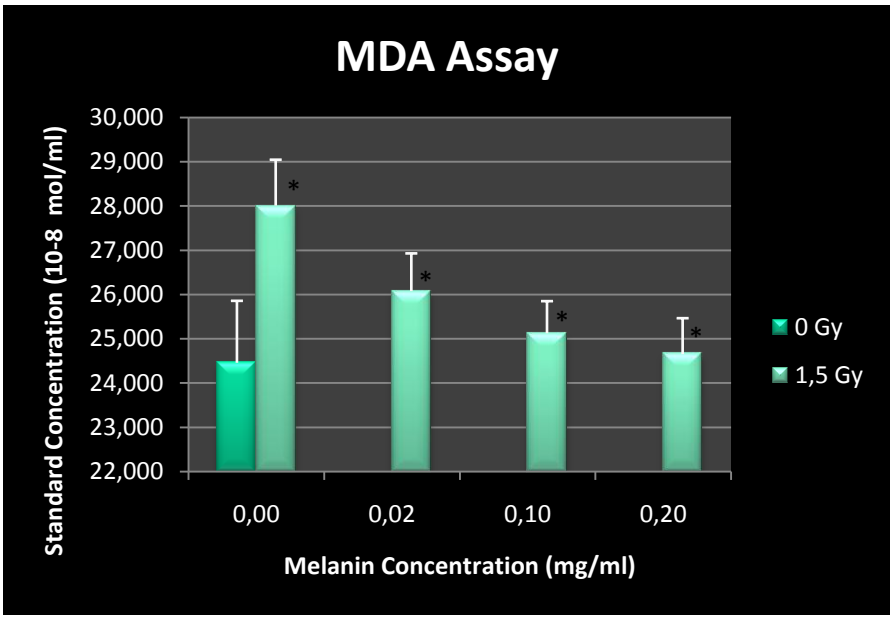

Fig. 30– MDA assay results in B16-F1 cells irradiated at 1.5Gy of gamma radiation for different concentrations of melanin added in culture medium. (*) p<0.01 between different melanin concentrations and compared to control (Student's t-test).

In order to investigate the pattern of melanin modulation for radiation damage with different intracellular concentrations of melanin, B16-F1 cells were incubated in Ham F10 media (Sigma-Aldrich, St Louis USA), with low and high concentration of melanin precursor, tyrosine. Hams F-10 medium was chosen for its low L-tyrosine content. Final concentrations used were the following: 0.01 mM concentration of L-tyrosine (1T- 0.01 mM tyrosine in the original Ham´s F-10 medium) and 40 times that concentration of L-tyrosine (40T – 0.4 mM) as described by Smit, et al. 1998. Calibration curve results are listed in Table 16 and depicted in Fig. 31 chart.

From these results a function was obtained by linear least square fitting method (see appendix 1: data analysis – linear least square fitting method), where fl corresponds to fluorescence and sc to standard concentration, σ_a is the uncertainty of parameter a and σ_b the uncertainty of parameter$b$. The function obtained was inverted to obtain concentration in function of fluorescence. Uncertainty of measurement was calculated using uncertainty propagation method (see appendix 1: data analysis – uncertainty propagation).

$$fl = 8.389 + 83.015sc$$

$$\sigma_a = 0.0.483$$

$$\sigma_b = 0.991$$

$$sc = \frac{fl - 8.389}{83.015}$$

$$\sigma_{sc}^2 = \left(\frac{\partial sc}{\partial fl}\right)^2 \sigma_{fl}^2 = \left(\frac{1}{83.015}\right)^2 \sigma_{fl}^2$$

Results at different melanin concentration are listed in Table 17 and depicted in Fig. 32 chart.

Table 16 - Calibration curve results - MDA assay for 1T and 40T L-tyrosine concentrations in culture medium. SD is the standard deviation.

Standard Concentration (10^{-6} mol/ml)	Mean	SD
0,00	6,817	0,594
0,25	30,312	0,944
0,50	50,069	0,200
1,50	130,345	2,478
2,50	196,114	5,169

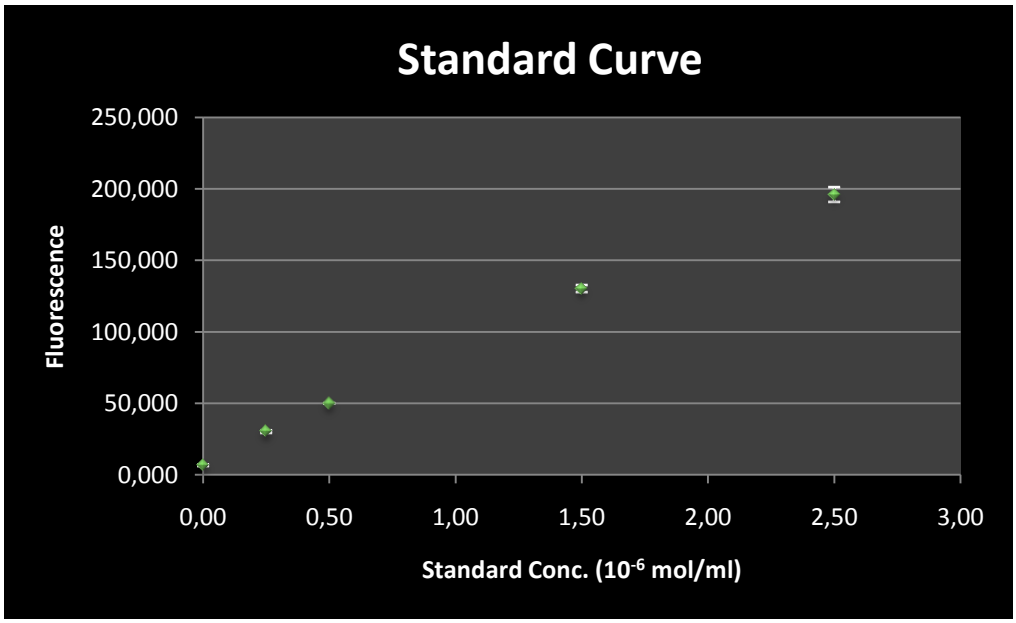

Fig. 31 - Calibration curve results - MDA assay for 1T and 40T L-tyrosine concentrations in culture medium.

Table 17- MDA assay results in B16-F1 cells irradiated at 1.5Gy of gamma radiation for 1T and 40T L-tyrosine concentrations in culture medium. σ_{SC} is the standard deviation in standard concentration.

Dose	Tyrosine concentration in medium	Concentration (10^{-8} mol/ml)	σ_{sc}
0 Gy	1T	35,939	1,245
1.5 Gy	1T	39,845	1,390
	40T	36,482	0,876

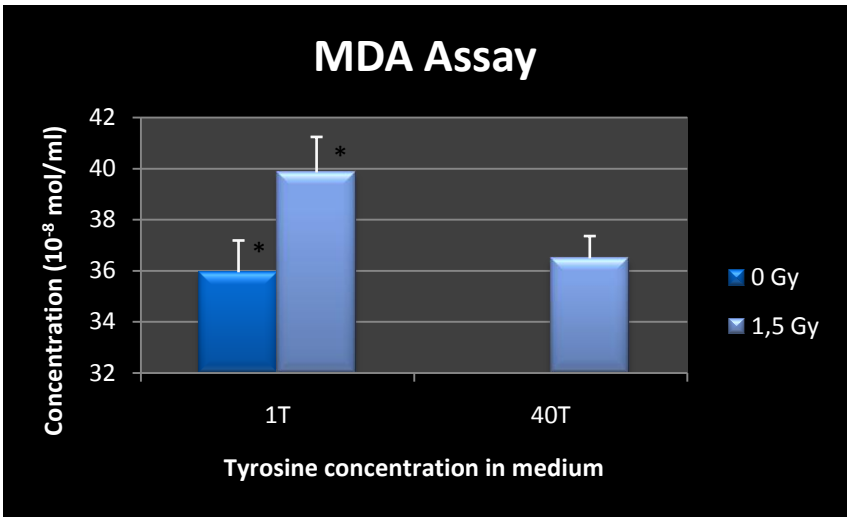

Fig. 32- MDA assay in B16-F1 cells irradiated at 1.5Gy of gamma radiation for 1T and 40T L-tyrosine concentrations in culture medium. (*) $p<0.05$[A1] compared to control (Student's t-test).

Discussion

Melanins are amorphous, irregular polymeric pigments present in most living organisms, generally responsible for the pigmentation of surface structure. They are insoluble in aqueous solution and some organic solvents (Ghannam 2003). In this work a 10 g/l melanin-DMSO solution was made. Mouse melanoma cells (B16-F1) were exposed to gamma radiation in the presence of different concentrations of extracellular melanin (added to the medium) and intracellular melanin (melanogenesis induction by its precursor tyrosine).

For choosing an irradiation dose, an initial dose-response study was performed. The endpoint chosen for the screening test was the cytokinesis blocked micronucleus (CBMN) assay, a measure of genotoxicity, was performed with irradiation doses of 0, 0.5, 1, and 2 Gy. The interpolated dose of 1.5 Gy was chosen for the remaining experiments because it provides an easily detectable effect, significantly different from un-irradiated control, while not relevantly inhibiting cell growth, allowing for the adequate quantification of melanin influence on radiation damage.

The selected irradiation dose was used in all the subsequent experiments: intracellular and extracellular variations of melanin concentration were induced in control and irradiated cells, and several endpoints of radiation damage were applied: cell viability by MTT assay, a non-specific measure of acute toxicity, oxidative stress by the quantification of lipoperoxydation products, expressed as malondialdehyde (MDA), and genotoxicity by the frequency of micronuclei in cytokinesis blocked binucleated cells (CBMN assay).

Differences in melanogenesis by using the different tyrosine concentration in media could be macroscopically observed (Fig. 33) by an obvious brown coloration of the supernatant on the 3rd day of culture in DMEM but no coloration in Ham's F10 medium.

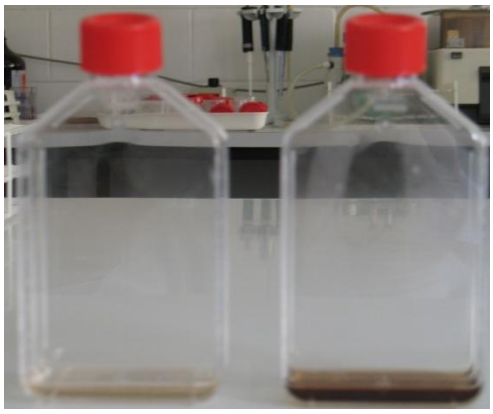

Fig. 33 – Soft-pink color in 3 days 1T Ham's F10 medium, dark-brown color in DMEM, consequence of B16-F1 melanin production.

The CBMN results show a significant decrease in the genetic lesion with increasing melanin concentration (all results significantly different from the control sample and from each other, $p<0.05$ Student's t-test), thus justifying the protective effect of melanin presence, by reducing genotoxicity of the gamma radiation. This protection may be achieved by reducing

the interaction of radiation with the target cells, through a shielding mechanism, or acting as a buffer molecule that reduces the yield of reactive and radicalar species.

MTT assay shows an increase in cell viability with increased melanin concentration, again pointing to a protective effect of melanin. This effect is marked in the melanin concentration range tested, with some overshoot of cell viability above the control sample values, which cannot exclude a possible presence of a non-specific confounding factor – potentially due to the absorbance of melanin itself, present in the supernatant medium. To obviate this problem, a reference wavelength was used, in an area of the visible spectrum where formazan does not absorb visible radiation, but melanin does (620 nm) and absorbance values at this wavelength were subtracted from the test wavelength (540 nm) absorbance (Matuszak and Wasilewska-Radwanska 2006): the dose-response trend remained unaltered, as it is shown. Also the protective effects of melanin are reproducible in all endpoints tested and so this is not an isolated finding. A subtle increase in cell viability was observed in 40T cells, although not statistically significant.

MDA values showed the same trend of dose-response as the previously described endpoints, adding strength to the model of melanin protective behaviour against ionizing radiation. Increasing melanin concentrations, both added melanin and induced melanogenesis, significantly decrease the concentration of lipoperoxydation products in the supernatant of gamma radiation exposed cells ($p<0.01$, Student's t-test) and therefore the level of oxidative stress experienced by the irradiated cells. In the melanogenesis induction experiments, the protective pattern was reproduced, with a strikingly significant decrease of lipoperoxydation products in the 40T medium irradiated samples, showing a level of oxidative stress not statistically different from control unirradiated cells. Considering that oxidative injury is regarded as a major pathway for ionizing radiation toxicity, melanin ability to counteract this effect is quite relevant in terms of radiation protection. In addition, results for lipoperoxydation assay are technically more likely to be over- rather than under-estimated: the specificity of the test based on MDA-TBA reaction is low, as TBA may react with several compounds other than MDA also derived from oxidation. Moreover, the treatment of biological samples to obtain the condensation product is usually carried out at high temperature (around 100^{o}C) and may generate further oxidation with obvious overestimation of results (Del Rio, Stewart and Pellegrini 2005). To overcome this limitation, the TBA-MDA complex is extracted from the reaction mixture with an organic solvent (1-butanol), and the quantification is made using this extract.

In summary, our integrated results strongly suggest that melanin plays an important role in protection against ionizing radiation.

Conclusions

The main conclusion drawn from the present study is that melanin may have an important role as a radioprotector for ionizing as well as non-ionizing radiation in living cells. This property may find applications, for example, in protecting bone marrow or gastrointestinal tract of cancer patients undergoing external beam radiation therapy, or possibly even individuals contaminated internally with radionuclides, from harmful local and systemic effects of ionizing radiation.

It is important to notice the remarkable capacity of melanin both to attenuate γ rays interaction by Compton Effect and, at same time, being capable of accept electrons of the resulting interaction, preventing hazardous secondary ionizations, and therefore further reducing oxidative stress in biological systems.

Future perspectives include testing of normal melanocytes, which have normal apoptotic pathways and allow an evaluation of the induction of apoptotic pathways by ionizing radiation in the presence and absence of melanin. This study could not be performed with B16-F1 cells due to the altered apoptosis

Because melanin is not soluble in aqueous solution, a future work could integrate a development of a delivery system capable of administering melanin systematically in form of nanoparticles such as nanospheres, stable in the water-based extracellular medium, in order to harvest melanin's protective properties without a necessary absorption of melanin by the living tissues. This development would make animal experiments possible. Another interesting future work may be conducting experiments on melanin behavior in cells irradiated with other qualities of ionizing radiation, like α particles, β particles and neutrons. This would further clarify melanin's response to particulate radiation, possibly expanding radioprotective potential to other applications, other scenarios and several different radiation emitters, including radioprotection applications in nuclear medicine therapy.

Bibliography

Amaro, João Abel. "Cancro Cutâneo - Factos e Números." *Associação Portuguesa de Cancro Cutânio.* 06 01, 2009. http://www.apcc.online.pt/ (accessed 06 01, 2009).

Amaro, João. "Cancro da Pele." *Associação Portuguesa de Cancro Cutâneo.* 06 01, 2009. http://www.apcc.online.pt/ (accessed 06 01, 2009).

Blettner, Maria, et al. "Mortality from cancer and other causes among male airline cockpit crew in Europe." *Int J Cancer*, 2003: 106, 946-952.

Bodenham, D. "A study of 650 observed malignant melanomas in the South West." *Ann R Coll Surg Engl*, 1968: 43 (4): 218-39.

Cohen, Philip J, Maja A Hofmann, Wolfram Sterry, and Robert A Schwartz. "Melanoma." Chap. Chapter 11 in *Skin Cancer: Recognition and Management 2nd ed.*, by Robert A Schwartz, 152-199. Maiden, MA: Blackwell Publishing, 2008.

Cooper, Samuel. *First lines of theory and practice of surgery.* London: Longman, Orme, Brown, Green and Longman, 1840.

Dadachova E, Bryan RA, Huang X, Moadel T, Schweitzer AD, et al. "Ionizing radiation changes the electronic properties of melanin and enhances the growth of melanized fungi." *PLoS ONE 2(5)*, 2007: e457. doi:10.1371/journal.pone.0000457.

Del Rio, Daniele, Amanda J Stewart, and Nicoletta Pellegrini. "A review of recent studies on malondialdehyde as toxic melecule and biological marker of oxidative stress." *Nutrition, Metabolism & Cardiovascular Diseases*, 2005: 15, 316-328.

Dousset, JC, M Trouilh, and MJ Foglietti. "Plasma malondialdehyde levels during myocardial infarction." *Clin Chim Acta*, 1983: 129: 319-322.

Fenech, Michael. "The in vitro micronucleus technique." *Mutation research*, 2000: 81-95.

Feng, Zhaohui, Wengwei Hu, Lawrence J Marnett, and Moon-shong Tang. "Malondialdehyde, a major endogenous lipid peroxidation product, sensitizes human cells to UV- and BPDE-induced killing and mutagenesis through inhibition of nucleotide excision repair." *Mutation Research*, 2006: 601, 125-136.

Fink, Cristopher A, and Michael N Bates. "Melanoma and ionizing radiation: is there a causal relationship?" *Radiation Research*, 2005: 164, 701-710.

Forshier, Steve. *Essentials of Radiation Biology and Protection.* Canada: Delmar, a division of Thomson Learning, Inc., 2002.

Ghannam, Magdy M. "Effect of gamma irradiation on some biophysical properties of melanin." *Egyptian Journal Of Biophysics* 9 (2003): 255-267.

Goulart de Medeiros, Margarida. *Genotoxicity of Chromium Compounds - Comparative Study in Leather Tanning.* Dissertation, Lisbon: FFUL, 2003.

Gregoire, O, and M R Cleland. "Novel approach to analyzing the carcinogenic effect of ionizing radiations." *Int. J. Ratiat. Biol.* Vol 82, No. 1 (January 2006): 13-19.

Gundestrup, Maryanne, and Hans H Storm. "Radiation-induced acute myeloid leukaemia and other cancers in commercial jet cockpit crew: a population cohort study." *The Lancet*, 1999: 2029-2031.

Haldorsen, Tor, Jon B Reiten, and Ulf Tveten. "Cancer incidence among Norwegian airline cabine attendants." *International Journal of Epidemiology*, 2001: 30, 825-830.

Harrison's. *Principles of Internal Medicine.* 16. Edited by Kasper, Braunwald, Fauci, Hauser, Longo and Jameson. New York: McGraw-Hill, 2005.

Howell, RC, AD Schweitzer, A Casadevall, and EA Dadachova. "Chemosorption of radiometals of ineterest to nuclear medicine by synthetic melanins." *Nucl Med Biol.*, 2008: 35(3): 353-357.

Ibelgaufts, Horst. *Horst Ibelgaufts' COPE: Cytokines & Cell Online Pathfinder Encyclopaedia.* 2008. http://www.copewithcytokines.de/cope.cgi?key=MTT%20assay (accessed 01 2009).

Langner, I, et al. "Cosmic radiation and cancer mortality among airline pilots: results from a european cohort study (ESCAPE)." *Radiat Environ Biophys*, 2004: 42: 247-256.

Lim, M K. "Cosmic rays: are air crew at risk?" *Occup Environ Med*, 2002: 59: 428-433.

Liu, Y, L Hong, VR Kempf, k Wakamatsu, S Ito, and JD Simon. "Ion-exchange and adsorption of Fe(III) by Sepia melanin." *Pigment cell research / sponsored by the European Society for Pigment Cell Research and the International Pigment Cell Society*, 2004: 17 (3): 262–9.

Marnett, Lawrence J. "Lipid peroxidation - DNA damage by malondialdehyde." *Mutation research*, 1999: 424, 83-95.

Marnett, Lawrence J. "Oxy radicals, lipid peroxidation and DNA damage." *Toxicology*, 2002: 181-182, 219-222.

Matuszak, Zenon, and M. Wasilewska-Radwanska. "Optical Properties of Melanin Solutions. Estimation of Polymer Particles Size." *Proceedings of the Symposium on Photonics Technologies for 7th Framework Program.* Wroclaw, Poland, 2006. 533-537.

"melanoma. [Photograph]." *Encyclopædia Britannica.* http://www.search.eb.com/eb/art-56764 (accessed 2009 11, February).

Mosmann, T. "Rapid colorimetric assay for cellular growth and survival: application to proliferation and cytotoxicity assays." *Journal of immunological methods*, 1983: 65: 55-63.

Nicholas, Joyce S, et al. "Cosmic radiation and magnetic field exposure to airline flight crews." *American Journal of Industrial Medicine*, 1998: 34: 574-580.

OECD. "Draft proposal for a new guideline 487: In Vitro Micronucleus Test." *OECD guideline for the testing of chemicals*, December 21, 2006.

Pukkala, E, et al. "Cancer incidence among 10,211 airline pilots: a nordic study." *Aviation, Space and Environmental Medicine* Vol 74, No. 7 (July 2003): 699-706.

Rafnsson, Vilhjálmur, Jón Hrafnkelsson, and Hrafn Tulinius. "Incidence of cancer among commercial airline pilots." *Occup Environ Med*, 2000: 57: 175-179.

Ribas dos Santos, Fernado. "Cancro Cutâneo." *Associação Portuguesa de Cancro Cutâneo.* 06 01, 2009. http://www.apcc.online.pt/ (accessed 06 01, 2009).

Scudiero, Dominic A, et al. "Evaluation of a suluble tetrazolium/formazan assay for cell growth and drug sensitivity in culture using human and other tumor cells." *Cancer Research*, 1988: 48, 4827-4833.

Smit, Nico P. M., et al. "Increased Melanogenesis is a Risk Factor for Oxidative DNA Damage - Study on Cultured Melanocytes and Atypical Nevus Cells." *Photochemistry and Photobiology*, 2008: 84: 550–555.

Smit, Nico P.M., et al. "Variations in melanin formation by cultured melanocytes from different skin types." *Arch Dermatol Res*, 1998: 290: 342-349.

Urteaga, Oscar, and George Pack. "On the Antiquity of Melanoma." *Cancer*, 1966: 19(5): 74-108.

web-books.com. 02 11, 2009. http://www.web-books.com/eLibrary/Medicine/Physiology/Skin/Skin.htm.

World Health Organization. *World Cancer Report 2008.* Edited by Peter Boyle and Bernard Levin. Lyon: IARC Press, 2008.

World Heath Organization. *Pathology and Genetics of Skin Tumors.* Edited by Philip E LeBoit, Günter Burg, David Weedon and David Sarasin. Lyon: IARC Press, 2006.

Zeeb, Hajo, et al. "Mortality from cancer and other causes among airline cabine attendants in Europe: a collaborative cohort study in eight countries." *Am J Epidemiol*, 2003: 158: 35-46.

Appendix 1

Data analysis

Propagation of Uncertainty

Being f a function of N varying parameters, $f(a_1, a_2, \dots, a_N)$. As known,

$$df = \sum_{k=1}^{N} \frac{\partial f}{\partial a_k} dx_k$$

i.e. if $a_k \to a_k + \delta a_k$, $f \to f + \delta f$. Moreover,

$$\delta^2 f = \sum_{k}^{N} \frac{\partial f}{\partial a_k} \frac{\partial f}{\partial a_j} \delta a_k \delta a_j$$

If $\{a_k\}$ values were the result of direct or indirect measurements, those values will be affected by statistical floating, translated in measurement uncertainty; which will be called σ_{a_k}. Propagation of uncertainty (or propagation of error) is the effect of variables' uncertainties (or errors) on the uncertainty of a function based on them. When the variables are the values of experimental measurements they have uncertainties due to measurement limitations which propagate to the combination of variables in the function.

The uncertainty (or error) should be:

$$\sigma_f^2 = \sum_{K=1}^{N} \left(\frac{\partial f}{\partial a_k} \right)^2 \sigma_{a_k}^2$$

Where $\sigma_{a_k}^2$ is the uncertainty of a_k.

Linear Least Square Fitting Method

The problem to know the best values of function parameters to describe a whole of measurements is normally called *fit.* The most common method consists in considering that best parameter estimative is that that minimize discrepancy between predicted values by function, $f(x_k)$, and measured values f_k.

Linear least square in statistic corresponds to the maximum likelihood estimate for a linear regression with normally distributed error. The goals of linear least squares are to extract predictions from the measurements and to reduce the effect of measurement errors.

If function represents a straight line, $y = a + bx$, fitting has a simple, analytical solution. When each measurement has different uncertainty from the other measurements the parameters *a* and *b* and respective uncertainties, σ_a and σ_b, are given by:

$$\gamma = \sum_i \frac{x_i^2}{\sigma_i^2} \sum_i \frac{1}{\sigma_i^2} - \left(\sum_1 \frac{x_i}{\sigma_i^2} \right)^2$$

$$a = \frac{1}{\gamma} \left[\sum_i \frac{x_i^2}{\sigma_i^2} \sum_i \frac{y_i}{\sigma_i^2} - \sum_i \frac{x_i}{\sigma_i^2} \sum_i \frac{x_i y_i}{\sigma_i^2} \right]$$

$$b = \frac{1}{\gamma} \left[\sum_i \frac{x_i^2 y_i^2}{\sigma_i^2} \sum_i \frac{1}{\sigma_i^2} - \sum_i \frac{x_i}{\sigma_i^2} \sum_i \frac{y_i}{\sigma_i^2} \right]$$

$$\sigma_a^2 = \frac{1}{\gamma} \sum_i \frac{x_i^2}{\sigma_i^2}$$

$$\sigma_b^2 = \frac{1}{\gamma} \sum_i \frac{1}{\sigma_i^2}$$

Appendix 2

Experimental Protocols

1. Micronuclei in cytokinesis blocked B16-F1 cells

Adapted from Goulart de Medeiros, 2003.

Cell cultures

1. Seed 1×10^5 cells in 5 cm diameter sterile Petri dishes and complete to 5 ml DMEM supplemented with 10% FBS (Sigma, St Louis, MO, USA), 1% penicillin + streptomycin.

2. Incubate at 37ºC, 5% CO_2.

3. At 24h of incubation perform irradiation procedure.

4. At 44h of incubation, add 100 µl of cytochalasin-B (Sigma, St. Louis, MO, USA) to a final concentration of 12.5 µM. (6 µg/ml, stock solution 8.34 mM prepared in DMSO).

Preparation of slides

1. After a total of 72 hours of culture, harvest cells by trypsination and centrifugation 1500 rpm, 10 minutes, at room temperature.

2. Wash twice with RPMI 1640 (pH 7.2), supplemented with 2% FBS.

3. Centrifuge for 7 minutes at 800 rpm, room temperature.

4. Remove supernatant, loosen pellet and subject cells to a mild hypotonic treatment, consisting of KCl 0.075M solution, for 2 min.

5. Centrifuge for 5 minutes at 800 rpm.

6. Remove supernatant and loosen pellet.

7. Place small drops of cell pellet in clean dry slides, and perform smears.

8. Air dry slides overnight.

9. Fix with freshly prepared ice-cold methanol/acetic acid (3:1) for 20 min.

10. Allow to dry and stain with 4% Giemsa in 0.01 M phosphate buffer pH 6.8 for 8 min.

11. Close the slides with Entellan® (Merck, Darmstadt, Germany).

2. MTT assay

Adapted from (Mosmann 1983)

1. Seed 100 µl (5 x 10^4) cells on each well of a 96-well plate. To avoid evaporation, do not use outer lines and columns of 96-well plate.

2. Incubate at 37ºC, 5% CO_2.

3. At 24h of incubation perform irradiation procedure.

4. At 48h of incubation add to each well 10 µl of MTT (0.5 mg/ml final concentration)

5. At 51h add 100 µl of DMSO to each well.

6. At 72h perform reading with Rosys Anthos 2010 multiwell reader spectrophotometer at 540nm (test wavelength) and 620nm (reference wavelength).

3. Determination of lipoperoxidation products by the MDA-TBA assay

(Adapted from Dousset *et al.*, 1983 and Goulart de Medeiros, 2003)

Standards

Tetramethoxipropane (Fluka AG, Buchs, Germany): dilute in dH_2O to final concentrations of 0.25 to 2.5 µM.

Blank: reaction mixture using dH_2O as "sample".

Thiobarbituric acid reagent

1. Add 400 mg thiobarbituric acid (TBA) (AppliChem BioChemica, Darmstadt, Germany) to 18 ml of 2N NaOH.

2. Adjust pH 7.4 with 7% perchloric acid.

3. Complete volume of 50 ml with dH_2O (solution A).

4. Add 2 volumes of Solution A to 1 volume of 7% perchloric acid (TBA reagent).

Reaction with thiobarbituric acid

1. Pipette triplicate aliquots of 1 ml post-irradiation (2-3 hours after irradiation) medium into screw-cap, heat resistant glass tubes, containing 25µl of BHT 0.2% in absolute alcohol.

2. Add 1.5 µl of freshly prepared TBA reagent.

3. Close the tubes tightly, vortex, and place in a boiling bath for ten minutes.

4. Cool down to room temperature.

5. Add 3 ml 1-butanol to each tube, close the tube tightly and vortex thoroughly.

6. Centrifuge for 15 minutes at 4000 rpm.

Quantification

Carefully remove each organic phase into measurement cuvette, mix and measure fluorescence of the solution at 515 nm excitation, 553 nm emission (Shimadzo RF-5000 Spectrofluorophotometer).